CARBON DIOXIDE CAPTURE FROM FLUE GAS USING DRY REGENERABLE SORBENTS

QUARTERLY TECHNICAL PROGRESS REPORT

Reporting Period: January 1, 2002 to March 31, 2002

by
David A. Green
Brian S. Turk
Raghubir P. Gupta
William J. McMichael
Douglas P. Harrison*
Ya Liang*

DOE Cooperative Agreement No. DE-FC26-00NT40923

Submitted by:

Research Triangle Institute
Post Office Box 12194
Research Triangle Park, NC 27709-2194

*Louisiana State University
Department of Chemical Engineering
Baton Rouge, LA 70803

April 2002

DISCLAIMER

TABLE OF CONTENTS

Page

List of Figures iv
List of Tables v

1.0 EXECUTIVE SUMMARY 1

2.0 INTRODUCTION 1

3.0 EXPERIMENTAL 2
3.1 Electrobalance Testing at LSU 2
3.1.1 Sorbents Used 2
3.1.2 Previous Experimental Results 2
3.1.3 Experimental Conditions 3
3.2 Fixed Bed Testing at LSU 4
3.3 Attrition Testing 4
3.4 Thermogravimetric Testing at RTI 4
3.5 Fluidized-Bed Reactor Testing at RTI 4

4.0 RESULTS AND DISCUSSION 4
4.1 Electrobalance Testing at LSU 4
4.1.1 Addition of Water Prior to Carbonation 4
4.1.2 Five-cycle Trona Tests 5
4.2 Fixed Bed Reactor Tests at LSU 10
4.3 Attrition Testing Results 13
4.4 Fluidized Bed Testing at RTI 14
4.5 Isothermal Thermogravimetry at RTI 16
4.5.1 Testing of Micronized Sodium Bicarbonate 16
4.5.2 Testing of Potassium Carbonate 16
4.6 Heat Transfer Analysis and Nonisothermal Testing at RTI 18
4.6.1 Shrinking Core Model 22

5.0 CONCLUSIONS AND FUTURE WORK 36

6.0 REFERENCES 37

LIST OF FIGURES

Figure **Page**

1 Smoothed electrobalance data for five carbonation cycles using trona T-200 and standard reaction conditions 5

2 Comparison of f(25) and f(150) for SBC #3 and trona T-2000 tests using standard reaction conditions 6

3 Smoothed electrobalance data for five carbonation cycles using trona T-200 and calcination in pure CO_2 at 200°C 7

4 Comparison of f(25) and f(150) for Trona T-200 using calcination at 120°C in He and 200°C in CO_2 8

5 Smoothed electrobalance data for five carbonation cycles using trona T-50 and 200°C calcination in CO_2 9

6 Comparison of f(25) and f(150) for Trona T-50 and T-200 using calcination at 200°C in CO_2 9

7 Mole percent CO_2 as a function of time in fixed-bed reactor test #6 10

8 CO_2 concentration (mole percent) as a function of time in second fixed-bed reactor test 12

9 CO_2 concentration (mole percent) as a function of time in a failed fixed-bed reactor test 12

10 Particle size distribution of SBC #5 prior to attrition testing 13

11 Particle size distribution of SBC #5 following attrition testing 14

12 Fluidized bed carbonation of potassium carbonate (3/11/02) 15

13 Temperature profile for fluidized bed carbonation of potassium carbonate 15

14 Calcination/carbonation of micronized sodium bicarbonate 16

15 Carbonation of potassium carbonate 17

16 Carbonation of calcined SBC #3 and dried potassium carbonate at 60°C 18

17 Effect of carbonation temperature using SBC grade #3 (for the formation of pure $Na_2CO_3 \bullet 3NaHCO_3$ dimensionless weight should equal 0.85) 19

18 Carbonation of equilibrium constants for the reaction 2/3 $Na_2CO_3 \bullet 3NaHCO_3 \rightarrow$ 5/3 $Na_2CO_3 + H_2O + CO_2$, calculated from two sources of thermodynamic data 20

19 Carbonation rate data obtained from Figure 17 21

20 Idealized thermogravimetric analyzer sample cup 22

21 Carbonation of SBC #3 at constant heating rate of 0.1°C/min 29

22 Carbonation of SBC #3 at constant heating rate of 0.2°C/min 29

23 Carbonation of SBC #3 at constant heating rate of 0.5°C/min 30

24 Carbonation of SBC #3 at constant heating rate of 1.0°C/min 30

25 Extent of carbonation of Na_2CO_3 to Wegscheider's salt as a function of time for the constant heating rate experiments 33

26 Determination of decomposition activation energy by means of ASTM E1541 35

LIST OF TABLES

Table		Page
1	Base Reaction Conditions	3
2	Davison Attrition Index Results	13
3	Comparison of the experimentally measured reaction times and reaction times computed using various models	28
4	Estimated equilibrium temperatures, Teq, obtained in four heating rate experiments summarized in Figure 5 through 8	31
5	Parameters use in constructing Figure 25	34
6	Temperatures corresponding to 20% conversion	34

1.0 EXECUTIVE SUMMARY

The objective of this project is to develop a simple, inexpensive process to separate CO_2 as an essentially pure stream from a fossil fuel combustion system using a regenerable, sodium-based sorbent. The sorbents being investigated in this project are primarily alkali carbonates, and particularly sodium carbonate and potassium carbonate, which are converted to bicarbonates, through reaction with carbon dioxide and water vapor. Bicarbonates are regenerated to carbonates when heated, producing a nearly pure CO_2 stream after condensation of water vapor.

This quarter, electrobalance tests conducted at LSU indicated that exposure of sorbent to water vapor prior to contact with carbonation gas does not significantly increase the reaction rate. Calcined fine mesh trona has a greater initial carbonation rate than calcined sodium bicarbonate, but appears to be more susceptible to loss of reactivity under severe calcination conditions.

The Davison attrition indices for Grade 5 sodium bicarbonate, commercial grade sodium carbonate and extra fine granular potassium carbonate were, as tested, outside of the range suitable for entrained bed reactor testing.

Fluidized bed testing at RTI indicated that in the initial stages of reaction potassium carbonate removed 35% of the carbon dioxide in simulated flue gas, and is reactive at higher temperatures than sodium carbonate. Removals declined to 6% when 54% of the capacity of the sorbent was exhausted.

Carbonation data from electrobalance testing was correlated using a shrinking core reaction model. The activation energy of the reaction of sodium carbonate with carbon dioxide and water vapor was determined from nonisothermal thermogravimetry.

2.0 INTRODUCTION

Fossil fuels used for power generation, transportation, and by industry are the primary source of anthropogenic CO_2 emissions to the atmosphere. Much of the CO_2 emission reduction effort will focus on large point sources, with fossil fuel fired power plants being a prime target. The CO_2 content of power plant flue gas varies from 4% to 9% (vol), depending on the type of fossil fuel used and on operating conditions. Although new power generation concepts that may result in CO_2 control with minimal economic penalty are under development, these concepts are not generally applicable to the large number of existing power plants.

This study is based on the use of a dry, regenerable sodium-based sorbent to remove CO_2 from flue gases. Sorbent regeneration produces a gas stream containing only CO_2 and H_2O. The H_2O may be separated by condensation to produce a pure CO_2 stream for subsequent use or sequestration. The primary reactions, based upon the use of sodium bicarbonate as the sorbent precursor and sodium carbonate as the reaction product are:

$$2NaHCO_3(s) \rightarrow Na_2CO_3(s) + CO_2(g) + H_2O(g) \quad (1)$$

and

$$Na_2CO_3(s) + CO_2(g) + H_2O(g) \rightarrow 2NaHCO_3(s) \quad (2)$$

Reaction (1) releases CO_2 and regenerates the sorbent, while Reaction (2) is used to capture CO_2. Several other solid products, intermediate between sodium carbonate and sodium bicarbonate, may also be produced under the anticipated reaction conditions. An intermediate compound, $Na_2CO_3 \bullet 3NaHCO_3$, forms at the reaction conditions of interest.

Analogous reactions (Reactions 3 and 4) take place within the potassium carbonate system:

$$2KHCO_3(s) \rightarrow K_2CO_3(s) + CO_2(g) + H_2O(g) \quad (3)$$

and

$$K_2CO_3(s) + CO_2(g) + H_2O(g) \rightarrow 2KHCO_3(s). \quad (4)$$

A compound salt of potassium carbonate and potassium bicarbonate is also thought to be of importance at the conditions of interest.

This report describes activities conducted between January 1, 2002 and March 31, 2002 by RTI and its subcontractors Louisiana State University (LSU) and Church and Dwight (C&D). Activities conducted this quarter include electrobalance (thermogravimetric analysis [TGA]) and fixed bed reaction studies at LSU, and TGA, fluidized-bed reactor testing, and thermodynamic and kinetic analyses at RTI. RTI also arranged for additional materials characterization testing.

3.0 EXPERIMENTAL

3.1 Electrobalance Testing at LSU

3.1.1 Sorbents Used

Thermogravimetric analysis (TGA) testing was conducted at LSU with sodium bicarbonate Grade 3 (SBC #3) and trona Grade T-200. Fixed bed testing was conducted with SBC #3. Selected properties of these materials, and other sorbents used (both as-received and following calcination), were reported in previous quarterly reports (Green et al., 2001a; b).

3.1.2 Previous Experimental Results

A summary of experimental results reported in the previous quarterly reports is presented below to provide background for the new results reported in this report. Although all samples were screened initially for reactivity, most of the testing has been conducted with SBC Grade #3 and with Trona T-50. Lack of reproducibility has plagued the T-50 results, and the following summary pertains primarily to SBC Grade #3.

- Both the initial reaction rate and achievable CO_2 capacity decrease with increasing carbonation temperature.

- The possible formation of by-products including $Na_2CO_3 \bullet H_2O$, $Na_2CO_3 \bullet NaHCO_3 \bullet 2H_2O$, and $Na_2CO_3 \bullet 3NaHCO_3$ at carbonation conditions of potential interest was proven by thermodynamic analysis.

- At constant temperature, the global reaction rate increases with an increase in both CO_2 and H_2O concentrations.

- Calcination in 100% CO_2 and 80% CO_2/20% H_2O at temperatures as high as 200°C did not cause a significant reduction in the sorbent activity in the subsequent carbonation cycle.

- Five-cycle tests using SBC #3 at standard carbonation and calcination conditions show a gradual loss in both reaction rate and final fractional carbonation with increasing cycle number.

- Results of five-cycle tests using SBC #3 at more severe calcination conditions of 200°C in atmospheres of pure CO_2 and 80%CO_2/20% H_2O were not significantly different than results at less severe standard calcination conditions.

- Initial fixed-bed reactor tests in which CO_2 concentration in the product gas was measured as a function of time produced questionable results. The problems probably resulted from the difficulty in vaporizing the H_2O feed at the low carbonation temperature of 70°C as well as improperly calibrated mass flow controllers.

3.1.3 Experimental Conditions

Base case reaction conditions for TGA tests at LSU are shown in Table 1. Results from experimental tests to examine the effect of carbonation and calcination temperature and gas composition are compared to results from these base case conditions. Base case carbonation gas composition approximates the flue gas composition resulting from the combustion of natural gas using 10% excess air. Base case calcination conditions (which may not be practical in commercial operation), were selected to minimize sorbent activity loss during regeneration.

Table 1. Base Reaction Conditions

Calcination	Temperature	120°C
	Pressure	1 atm
	Gas Composition	100% He
Carbonation	Temperature	70°C
	Pressure	1 atm
	Gas Composition	8 mol% CO_2 16 mol% H_2O
	Gas Flow Rate	76 mol% He 600 scc/min

The following experimental procedure is used in base case tests. An initial charge of approximately 70 mg of sorbent precursor is heated from room temperature to 100°C at a rate of 5°C/min and from 100°C to the final calcination temperature of 120°C at a rate of 1°C/min under flowing He. After calcination is complete (as indicated by constant weight), the temperature is decreased at a rate of 2°C/min still under He to the 70°C carbonation temperature. The gas composition is then changed to 8 mol% CO_2, 16 mol% H_2O, balance He flowing at 600 scc/min and carbonation is continued until the reaction rate approaches zero as indicated by constant weight. Appropriate changes in this procedure are made when carbonation and calcination temperatures and gas compositions are changed from the base case.

3.2 Fixed Bed Testing at LSU

The LSU fixed bed reactor system, described in the previous quarterly report (Green, et al., 2002) was used to conduct three tests. One preliminary two cycle test was conducted in which approximately 20 g of SBC #3 sorbent was calcined in He at 120°C and then carbonated in 8% CO_2, 16% H_2O, balance He at 70°C. These tests were used to explore the effects of humidification of the sorbent prior to introduction of simulated flue gas and to generate samples for analysis by X-ray diffraction and scanning electron microscopy.

3.3 Attrition Testing

A sample of commercial grade sodium carbonate was subjected to testing by ASTM Method D 5757-95, Determination of Attrition and Abrasion of Powdered Catalysts by Air Jets. The same material, as well as samples of SBC #5 potassium carbonate, were tested by the jet cup method for determination of Davison Index.

3.4 Thermogravimetric Testing at RTI

RTI conducted carbonation tests on potassium carbonate at 60°C for comparison to earlier testing with calcined sodium bicarbonate. Additional testing of potassium carbonate was conducted at 70 and 80°C. Micronized sodium bicarbonate, provided by Church and Dwight was calcined and tested for comparison of activity with SBC #3. Finally, non-isothermal tests of calcined SBC #3 at four different heating rates (0.1, 0.2, 0.5 and 1.0°C/min) were conducted in an attempt to determine the effective activation energy of the carbonation reaction.

3.5 Fluidized-Bed Reactor Testing at RTI

RTI made four attempts to conduct cyclic carbonation/calcination tests of potassium carbonate in the fluid bed reactor system. An attempt to add water to the top of the fluid bed, for cooling and to promote carbonation, resulted in plugging of the bed. One successful carbonation test was completed; excessive pressure drops, indicating poor fluidization and plugging prevented useful data acquisition in the remaining tests.

4.0 RESULTS AND DISCUSSION

4.1 Electrobalance Testing at LSU

4.1.1 Addition of Water Prior to Carbonation

A single-cycle test using SBC #3 in which H_2O was added to the He for 30 minutes prior to introduction of CO_2 was carried out. Otherwise, standard calcination and carbonation conditions were used. This early introduction of H_2O was based on comments at the January project review meeting at RTI suggesting that the presence of a pre-adsorbed H_2O film on the sorbent might increase carbonation rate. The test was conducted even though the adsorption of a significant amount of H_2O at the 70°C carbonation temperature was doubtful. Test results, expressed as f(25) and f(150) were not significantly different than obtained previously when CO_2 and H_2O were added simultaneously.

4.1.2 Five-cycle Trona Tests

Four five-cycle tests using trona, T-200 (three tests) and trona T-50 (one test), were carried out to provide comparison with previous multicycle results using SBC #3. Standard carbonation conditions were used in each test while calcination was performed either in He at 120°C or CO_2 at 200°C. The samples were sieved and particles in the 70-80 mesh size range were tested. While previous single-cycle test results using trona showed poor reproducibility, the problem was attributed to inability to obtain replicate split samples. Multi-cycle testing offered an opportunity to compare rates for the same sample.

Results of the five-cycle test using trona T-200 with standard carbonation and calcination conditions are shown in Figure 1, where dimensionless weight during the carbonation cycle is plotted versus time. Reproducibility of both reaction rate and final carbonation is quite good. Note that the dimensionless weight was effectively constant after about 75 minutes and tests were terminated before the 150-minute time period used previously to characterize carbonation capacity.

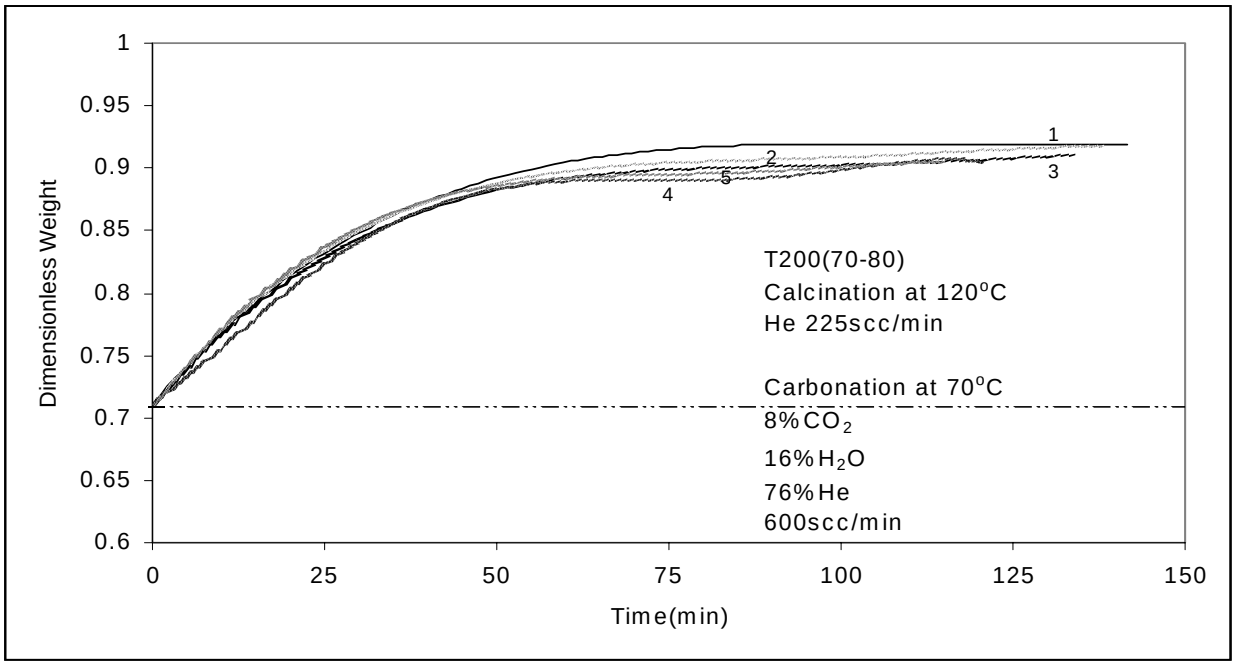

Figure 1. Smoothed electrobalance data for five carbonation cycles using trona T-200 and standard reaction conditions.

Results of multicycle tests using SBC #3 and Trona T-200 are compared in Figure 2 where f(25) and f(150) are plotted versus cycle number. The T-200 results shown in Figure 1 have been extrapolated to 150 minutes for comparison with the earlier SBC #3 results. In addition, the data points for SBC #3 represent the average of the three duplicate five-cycle runs reported

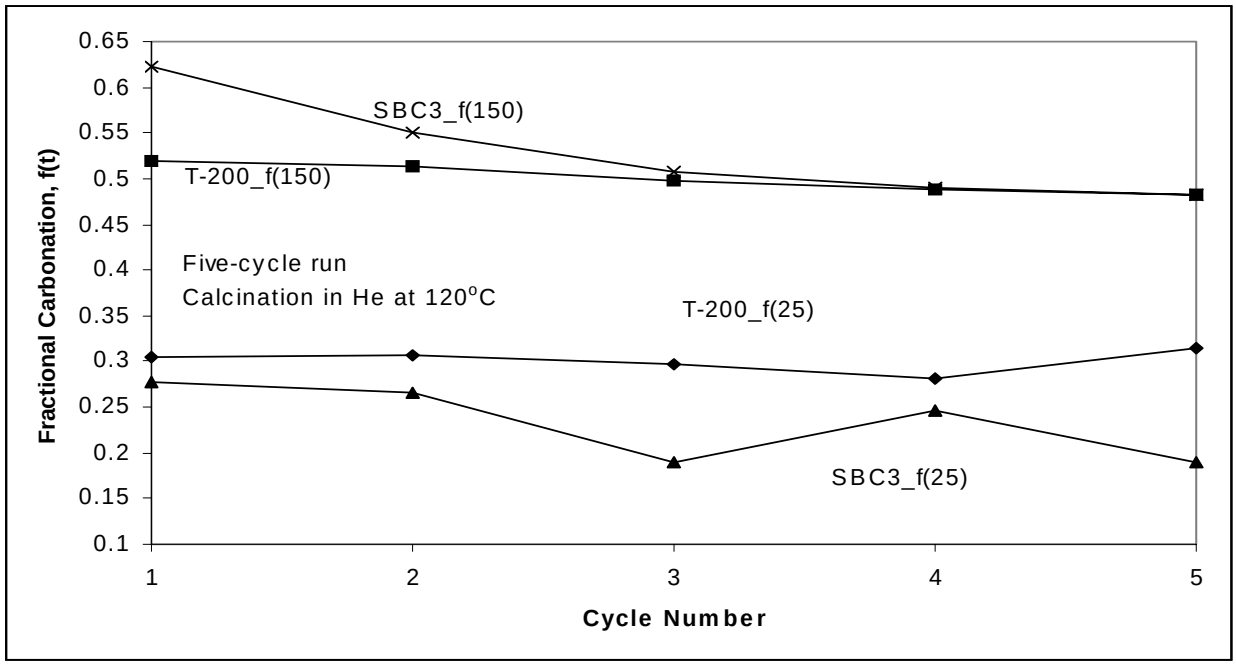

Figure 2. Comparison of f(25) and f(150) for SBC #3 and trona T-2000 tests using standard reaction conditions.

in the previous quarterly report (Green, et al., 2002). The parameter, f(t), for SBC #3 was calculated from

$$f(t) = \frac{m(t) - 0.631}{0.369} \tag{5}$$

where m(t) is the dimensionless weight at t (minutes).

f(t) for T-200 was calculated by

$$f(t) = \frac{m(t) - 0.711}{0.401} \tag{6}$$

Equation (6) reflects the different stoichiometry associated with trona as well as the presence of 2.5% impurities. The theoretical dimensionless weight corresponding to complete calcination is 0.711, while 0.401 is the theoretical dimensionless weight increase associated with complete carbonation.

The reaction rate for T-200, represented by f(25), is both greater and more consistent for than for SBC #3. For practical purposes, there is no decrease in f(25) with increasing cycle number. The capacity, represented by f(150), is initially smaller for T-200 but is effectively constant through the five cycles. By the third cycle there is no significant difference between the f(150) values for SBC #3 and T-200.

Dimensionless weight versus time results for the five-cycle test using T-200, with calcination at 200°C in pure CO_2, are shown in Figure 3. There is increased scatter between cycles compared to lower temperature calcination shown in Figure 1. In addition, both the f(25) and f(150) values, as shown in Figure 4, are significantly smaller than at the milder calcination conditions. Thus, it appears that the increased calcination temperature is significantly more harmful to T-200 than to SBC #3. The previous quarterly report (Green et al., 2002) showed that SBC #3 experienced relatively little decrease in performance associated with calcination in CO_2 at higher temperature. However, this conclusion must be tested further since different samples of T-200 were used in the two tests, and the problems in obtaining satisfactory reproducibility when using different trona samples have already been mentioned.

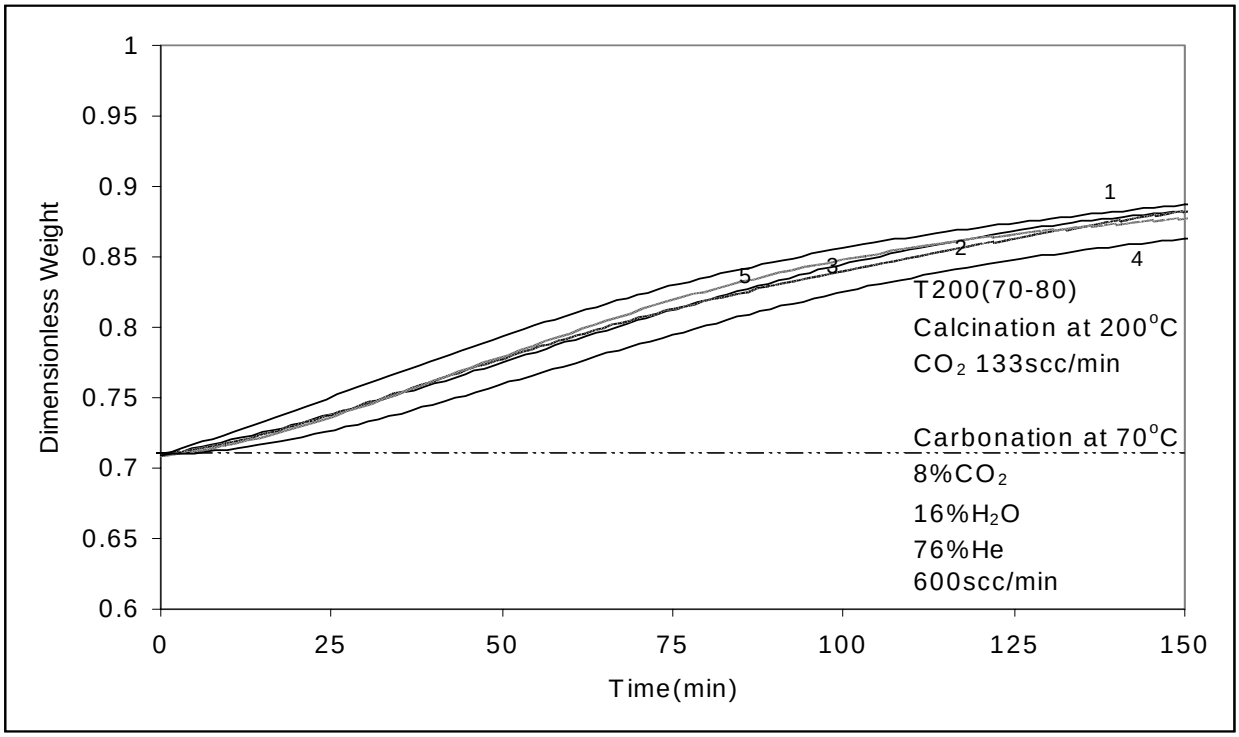

Figure 3. Smoothed electrobalance data for five carbonation cycles using trona T-200 and calcination in pure CO_2 at 200°C.

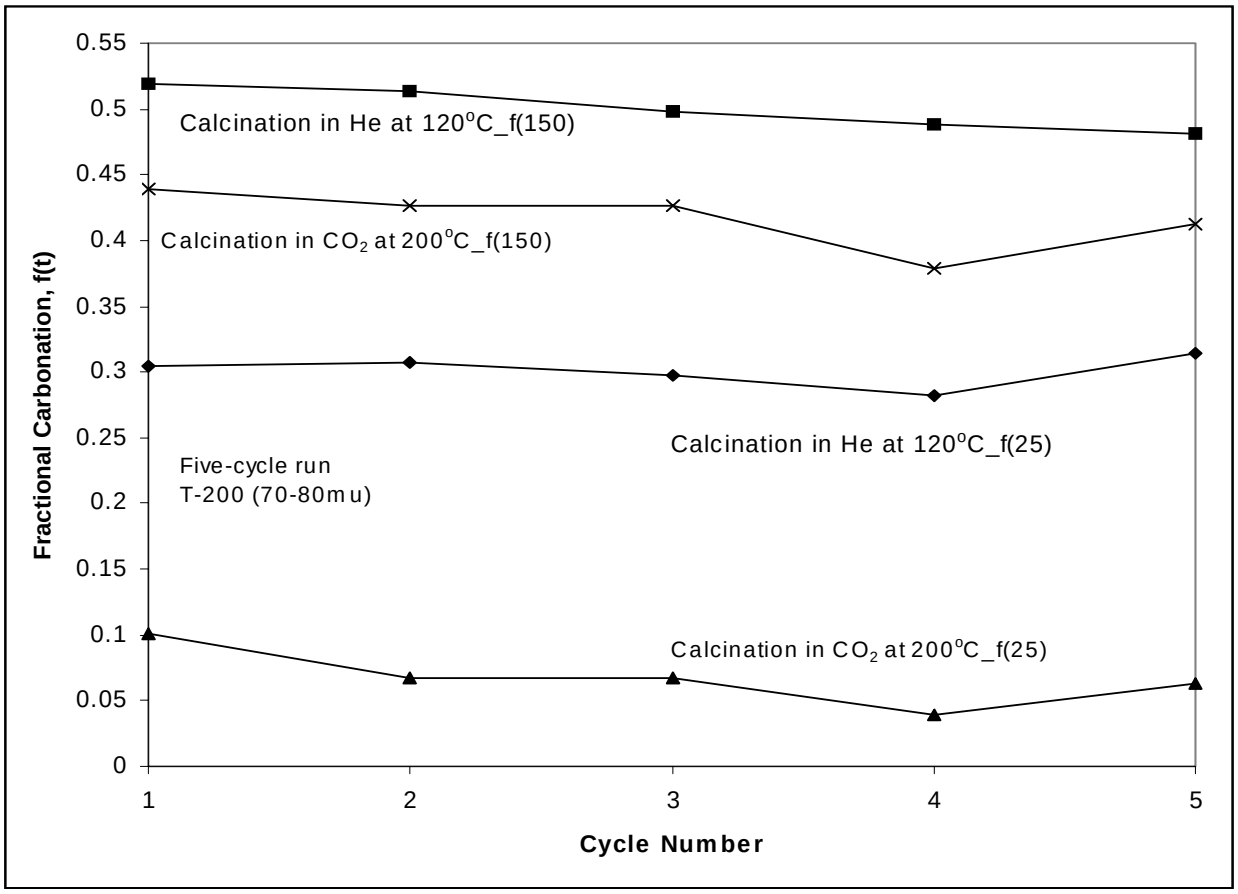

Figure 4. Comparison of f(25) and f(150) for trona T-200 using calcination at 120°C in He and 200°C in CO_2.

Trona T-50 was subjected to one five-cycle test using standard carbonation conditions, but with calcination at 200°C in CO_2. Dimensionless weight versus time results shown in Figure 5 are qualitatively similar to those in Figure 3 for T-200, at the same reaction conditions. There is only moderate variation between cycles which would be expected within experimental measurement limits.

Performance of T-50 and T-200 is compared in Figure 6 in terms of f(25) and f(150) as a function of cycle number. The parameter, f(t), was calculated for T-50 by Equation (7):

$$f(t) = \frac{m(t) - 0.723}{0.385} \tag{7}$$

Equation (7) also reflects the trona stoichiometry and the 6.5% impurities in T-50. This figure emphasizes the similarity between T-200 and T-50 results seen in Figures 3 and 5.

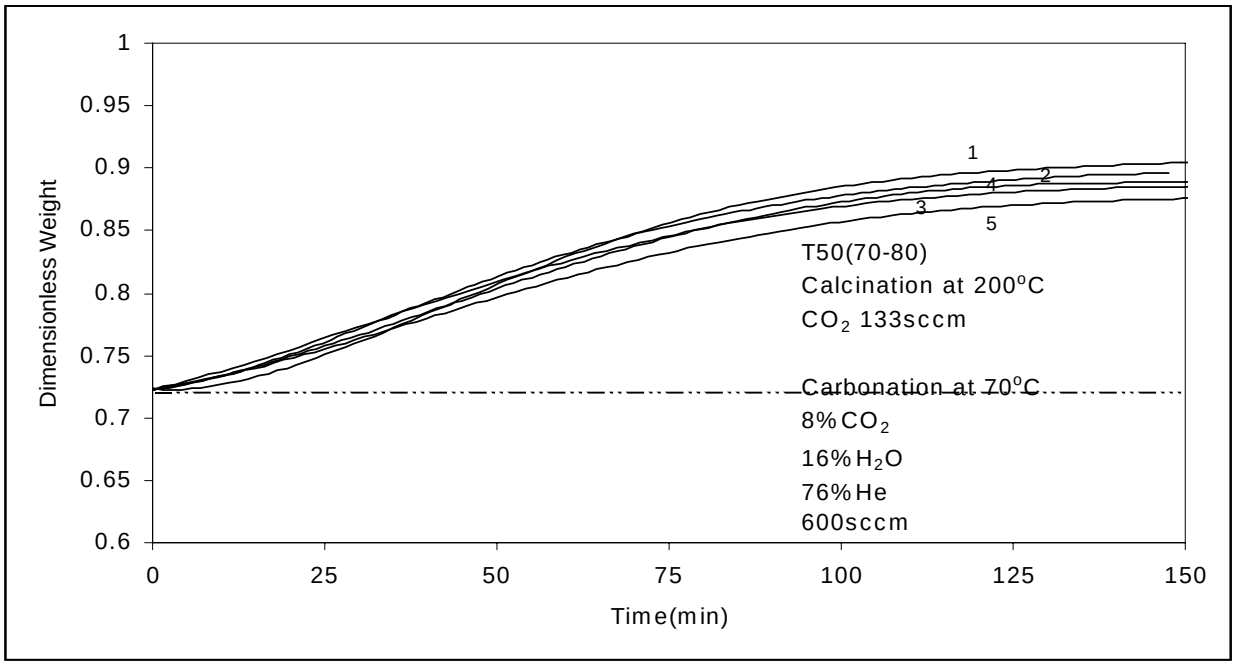

Figure 5. Smoothed electrobalance data for five carbonation cycles using trona T-50 and 200°C calcination in CO_2.

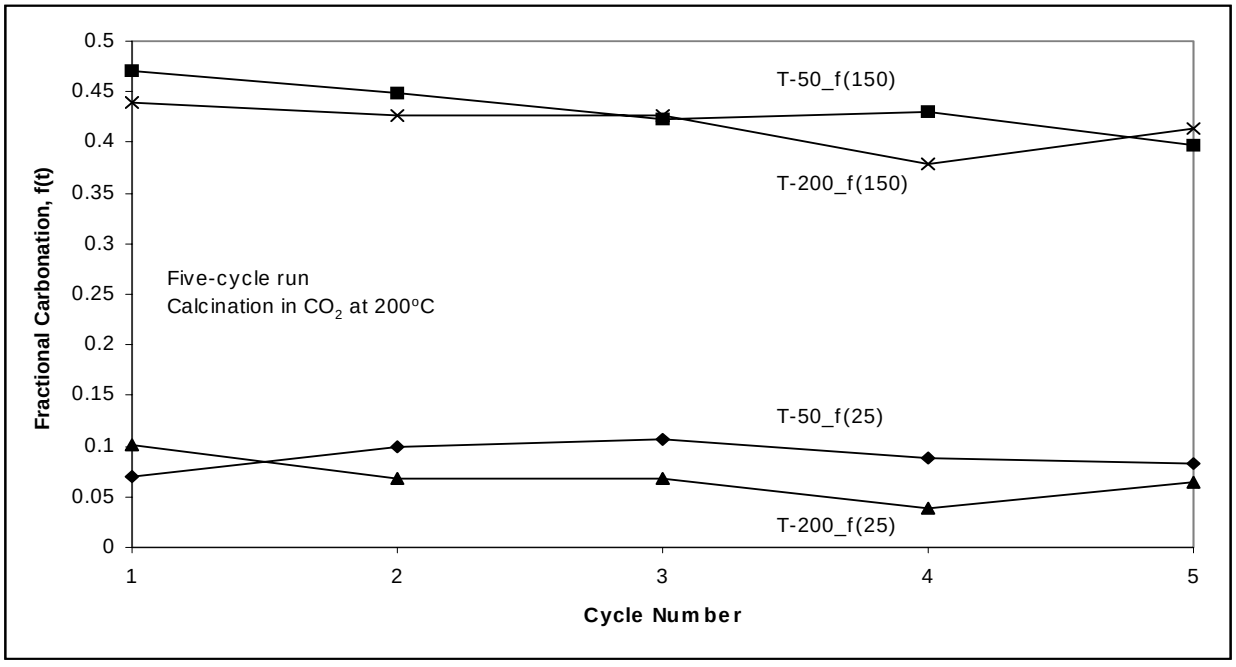

Figure 6. Comparison of *f(25)* and *f(150)* for trona T-50 and T-200 using calcination at 200°C in CO_2.

4.2 Fixed Bed Reactor Tests at LSU

Results of the initial fixed-bed reactor test were reported in the previous quarterly report (Green, et al., 2002). While this test proved that significant CO_2 removal could be achieved at reaction conditions of interest, the results were unsatisfactory in two important respects. Material balance closure was poor and CO_2 concentration in the product gas as a function of time did not exhibit the traditional breakthrough curve shape. The CO_2 concentration was high initially, decreased to a minimum, and then increased to a steady value. Failure to close the material balance was believed to be due to incorrectly calibrated mass flow controllers, while the problem with the CO_2 breakthrough curve was believed to be due to the difficulty in vaporizing H_2O at the low reaction temperature. It appeared that the high initial CO_2 concentration was due to the initial exposure of the sorbent to a H_2O-free mixture of CO_2 and N_2 for a period of time before water was vaporized to expose the sorbent to the mixture of CO_2 and H_2O needed for reaction.

As shown below, re-calibration of the mass flow controllers appeared to solve the material balance closure problem, and feeding a mixture of H_2O and N_2 for several minutes prior to the addition of CO_2 improved, but did not necessarily solve, the CO_2 breakthrough problem. Figure 7 shows the CO_2 concentration as a function of time during a first calcination, first carbonation, and second calcination of SBC #3. Standard carbonation and calcination gas compositions were used with the exception that an H_2O-N_2 mixture was fed during the first 30 minutes of carbonation before CO_2 was added. The total feed rate during carbonation was 300 scc/min. Initial calcination at 120°C was carried out during the first day and the sorbent was allowed to cool overnight to 70°C in N_2; carbonation and the second calcination occurred the next day.

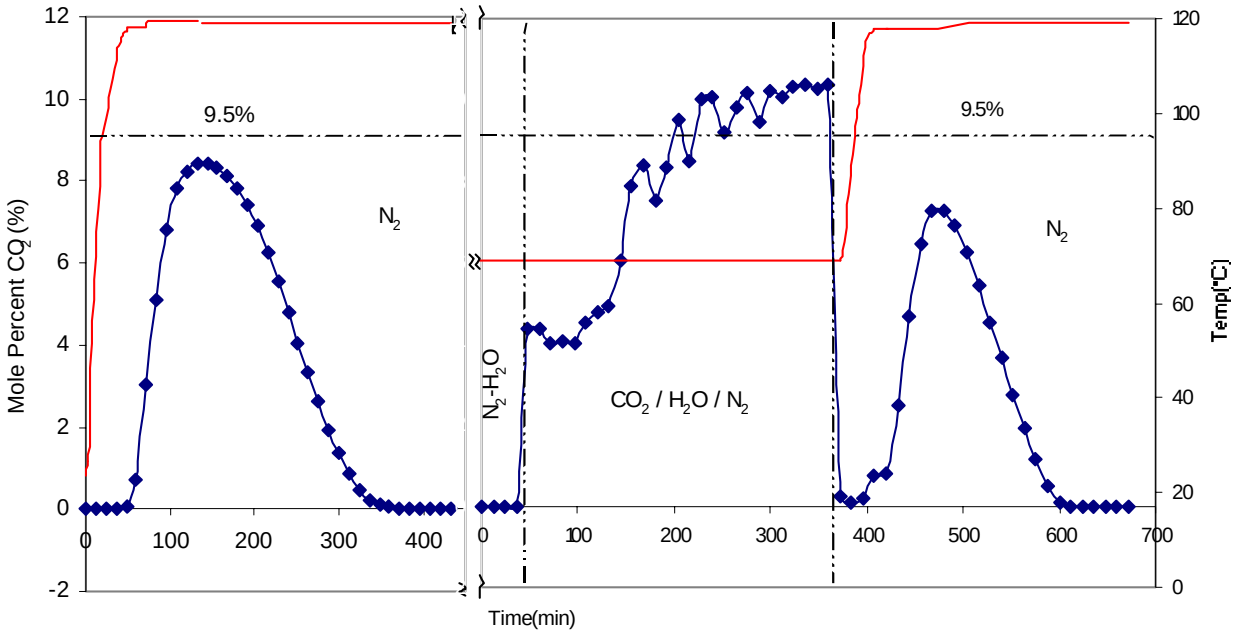

Figure 7. Mole percent CO_2 as a function of time in fixed-bed reactor test #6.

CO_2 concentration during the first calcination is shown is the left portion of Figure 7. The maximum CO_2 concentration of 8.4% was reached after about 140 minutes, and calcination was complete in about 350 minutes. Numerical integration of the area under the calcination curve showed that 0.155 mols of CO_2 were produced compared to a theoretical value of 0.150 mols associated with the 25.1 g initial charge of $NaHCO_3$. Thus it appears that the material balance closure problem was solved when the mass flow controllers were recalibrated.

In the carbonation portion of this test, shown as the middle portion of Figure 7, H_2O and He were fed for 30 minutes before CO_2 was added; the CO_2 concentration-time curve had the general appearance associated with a breakthrough curve. During the first 80 minutes of carbonation the CO_2 concentration was in the range of 4.0% to 4.9% (dry basis), corresponding to CO_2 removal in the range of 50% to 60%. The CO_2 concentration then increased to a steady-state value of about 10.3% (dry basis). This final concentration is somewhat higher than the theoretical 9.5% (dry basis) CO_2 corresponding to zero CO_2 removal. The jagged nature of the CO_2 breakthrough curve may be due to unsteady H_2O vaporization.

The right portion of Figure 7 corresponds to the second calcination cycle. In this second calcination the maximum CO_2 concentration was 7.2% and the area under the curve corresponded to 0.081 mols of CO_2 released. This corresponds to 52% of the theoretical capacity of the Na_2CO_3, and is reasonably consistent with the fractional carbonation values obtained during electrobalance tests.

Results from a second fixed-bed reactor test are shown in Figure 8. Reaction conditions were the same as for the test shown in Figure 7, except that the H_2O-N_2 mixture was fed for 60 minutes at the beginning of carbonation before adding CO_2. Based on the experimental results for the first calcination cycle, 0.164 mols of CO_2 were produced compared to a theoretical value of 0.152 mols. The CO_2 concentration was decreased to about 5.2% (dry basis) during the first 100 minutes of carbonation, corresponding to about 48% CO_2 capture. This is based on the low concentrations at the beginning and end of of the pre-breakthrough period, and ignores the peak in the middle. As before, this peak probably results from unsteady vaporization of H_2O. Once again the final CO_2 concentration during carbonation of 10.5% (dry basis) is somewhat higher than the theoretical value of 9.5%. The area under the CO_2 curve during the second calcination corresponds to 0.081 mols, or 49% of the CO_2 produced during the first calcination. This bed average value of 49% carbonation is also in reasonable agreement with electrobalance results.

The two fixed-bed reactor tests described above were completed during the initial portion of the quarter. Near the end of the quarter one more fixed-bed test was attempted; the results are shown in Figure 9. The experimental value of CO_2 produced during the initial calcination was 0.147 mols compared to a theoretical value of 0.150 mols based on the initial $NaHCO_3$ charge. Although a mixture of H_2O-N_2 was fed for 30 minutes at the beginning of carbonation, the results suggested an absence of H_2O during the first stages of carbonation. The CO_2 concentration showed an initial maximum, followed by a decrease, and then a gradual increase corresponding to breakthrough. This test was terminated after the first carbonation.

This result emphasizes the sensitivity of the fixed-bed reactor operation. If there is insufficient feed gas preheat, the H_2O will not be properly vaporized and no CO_2 removal will occur. Increasing the level of preheat may result in the gases being above the desired reaction temperature when first contacting the sorbent. This could also result in no CO_2 removal since the temperature window for the carbonation reaction is small.

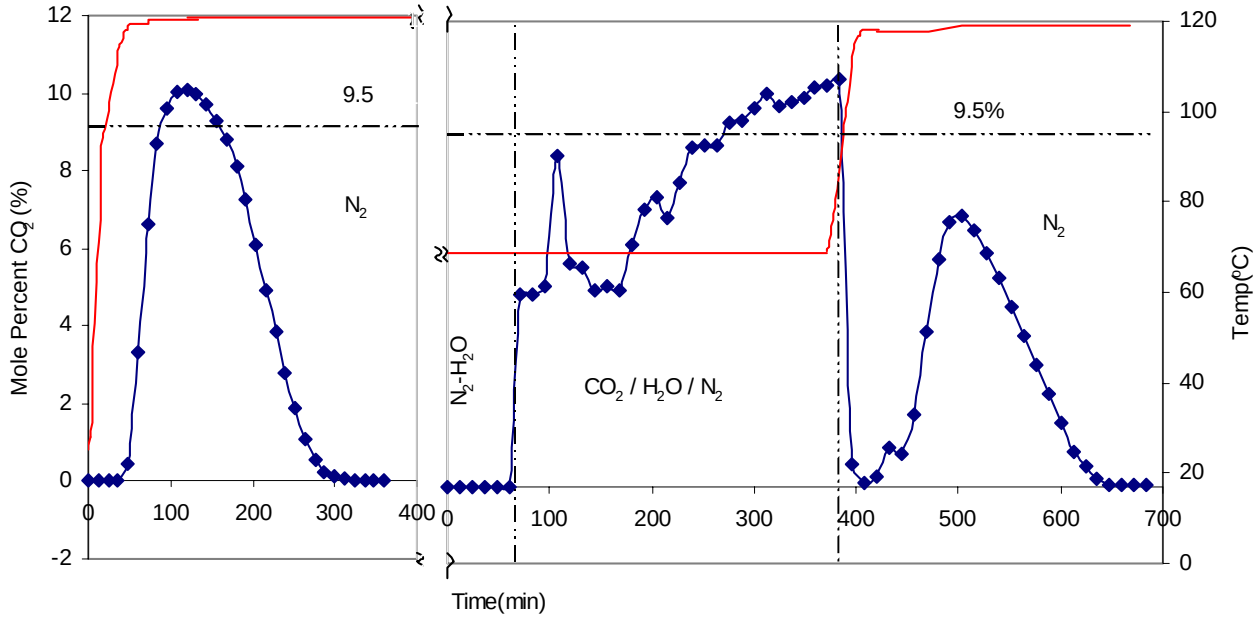

Figure 8. CO_2 concentration (mole percent) as a function of time in second fixed-bed reactor test.

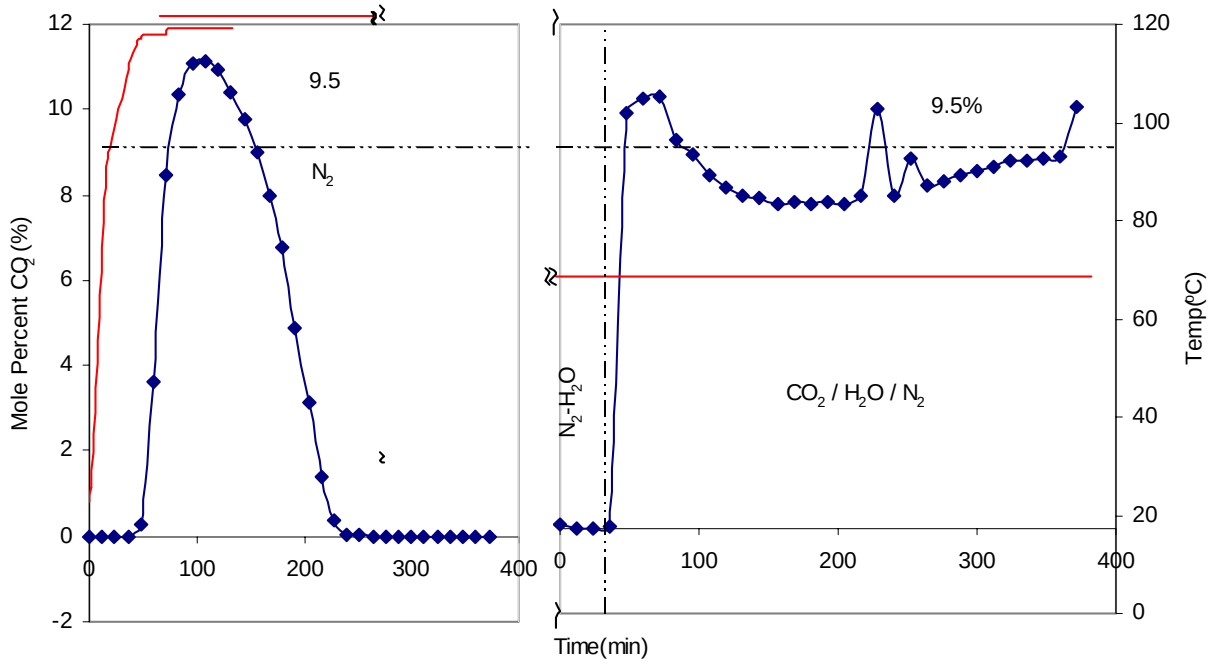

Figure 9. CO_2 concentration (mole percent) as a function of time in a failed fixed-bed reactor test.

Sorbent samples from two tests, those illustrated in Figures 7 and 9, were sent to RTI for subsequent transmittal to Church and Dwight for characterization in the coming quarter. One sample (Figure 7) should be essentially all Na_2CO_3 while the second (Figure 9) should be a mixture of Na_2CO_3 and $NaHCO_3$. These samples may confirm whether other reaction products such as $Na_2CO_3 \bullet H_2O$, $Na_2CO_3 \bullet NaHCO_3 \bullet 2H_2O$, and $Na_2CO_3 \bullet 3NaHCO_3$ are actually formed at standard carbonation conditions.

4.3 Attrition Testing Results

A sample of commercial grade sodium carbonate was subjected to air jet attrition testing (ASTM D 5757 -95) at RTI and found to have an attrition index of less than 2.0. This would suggest that this material may be a candidate for use in a transport reactor. This material, as well as samples of SBC #5, and potassium carbonate were subjected to jet cup attrition testing for determination of Davison Attrition Index (DAI) and found to perform poorly. Results of jet cup attrition tests are given in Table 2. Particle size distributions of SBC #5, before and after jet cup attrition testing are given in Figures 10 and 11. Recoveries of potassium carbonate were extremely low, indicating that this material was much more susceptable to attrition than the either the SBC #5 or the sodium carbonate. None of these materials have suitable attrition resistence for successful processing in entrained bed reactor systems.

Table 2. Davison Attrition Index Results.

Material	DAI
SBC #5	41
Sodium Carbonate (commercial)	>30
Potassium Carbonate (extra fine, anhydrous, granular)	>>30

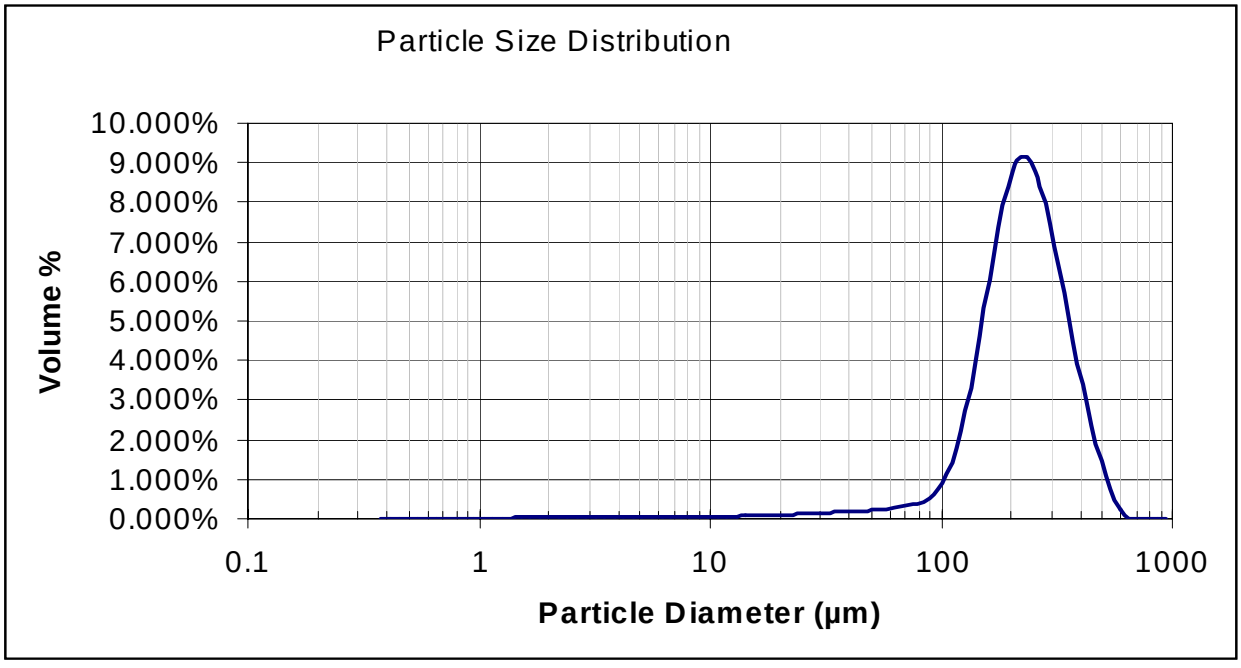

Figure 10. Particle size distribution of SBC #5 prior to attrition testing.

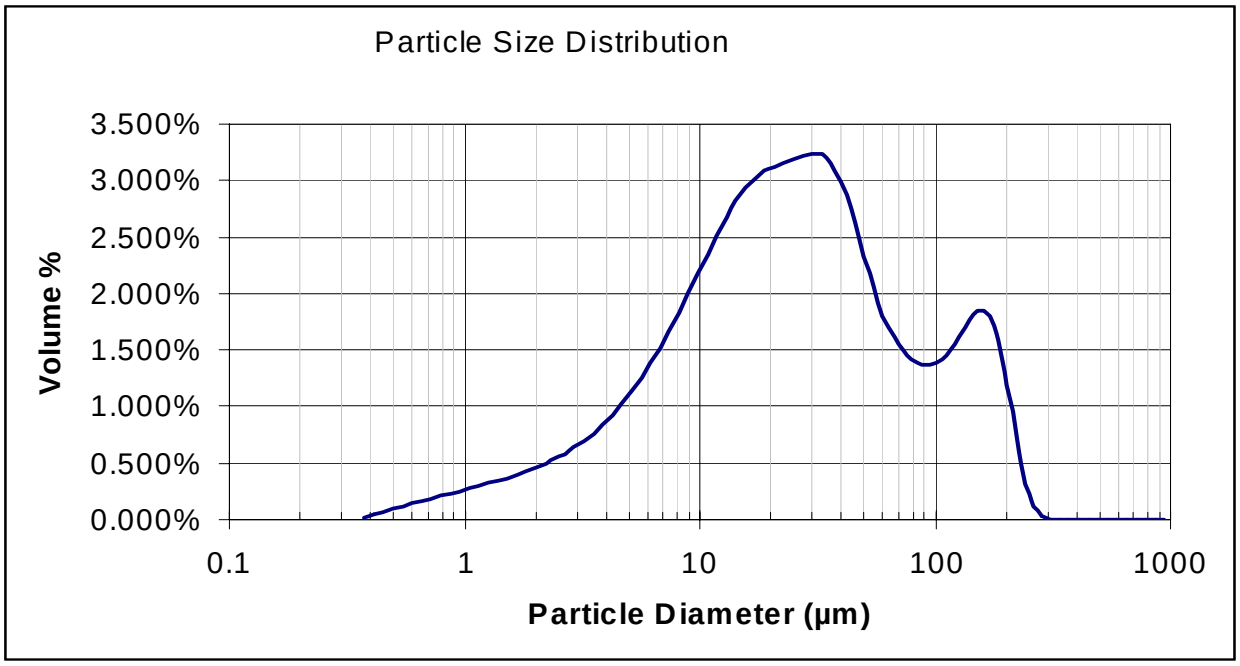

Figure 11. Particle size distribution of SBC #5 following attrition testing

4.4 Fluidized Bed Testing at RTI

Several attempts were made to conduct cyclic fluidized bed tests in the RTI fluidized bed reactor system. Problems were encountered with plugging of the bed, as indicated by an increase in differential pressure across the bed. Testing was conducted both with extra fine material and with analytical grade material (EM Science, Darmstadt, Germany). The bed plugged both during pre-drying in dry nitrogen, and during carbonation in nitrogen/oxygen/ carbon dioxide/steam mixtures. In general, the material is hygroscopic and tends to agglomerate during storage. One carbonation cycle was completed. Data are shown in Figure 12. The reactor temperature profile is shown in Figure 13. The reactor plugged up upon calcination following this carbonation cycle.

The test was conducted with 6.55% carbon dioxide and 6.14% water in the inlet gas. Carbon dioxide removal in the early stages of this test peaked at about 35% and remained above 15% for the first 30 minutes. The temperature in the bed increased rapidly due to the exothermic nature of the reaction. The fact that CO_2 removal continued to take place at these temperatures (peaking at about 110°C, averaged across the bed) suggests that potassium carbonate might have advantages over sodium carbonate for flue gas operations.

The CO_2 removal declined to about 6% after 280 minutes, at which point the sorbent bed was only 54% exhausted (based on conversion to potassium bicarbonate). The high initial removals may be indicative of reactivity in short residence time reactor systems such as transport reactors or entrained bed systems. On this basis, potassium carbonate may be a promising sorbent if problems related to agglomeration and attrition can be resolved.

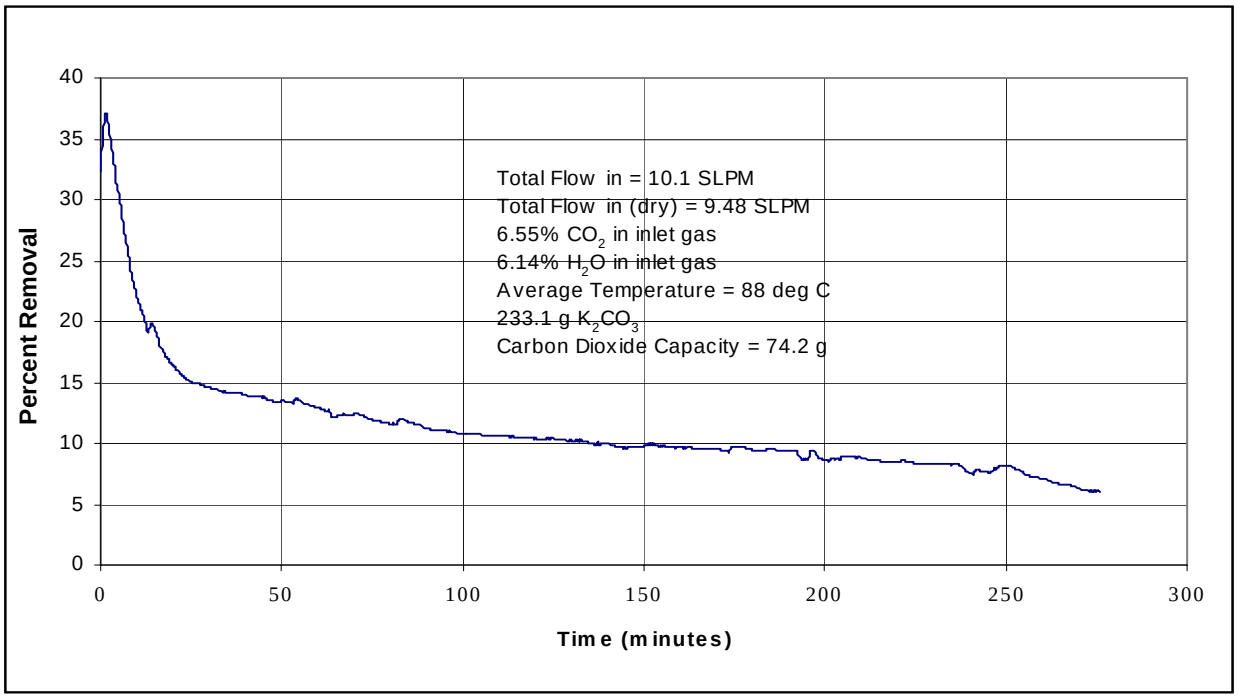

Figure 12. Fluidized bed carbonation of potassium carbonate (3/11/02).

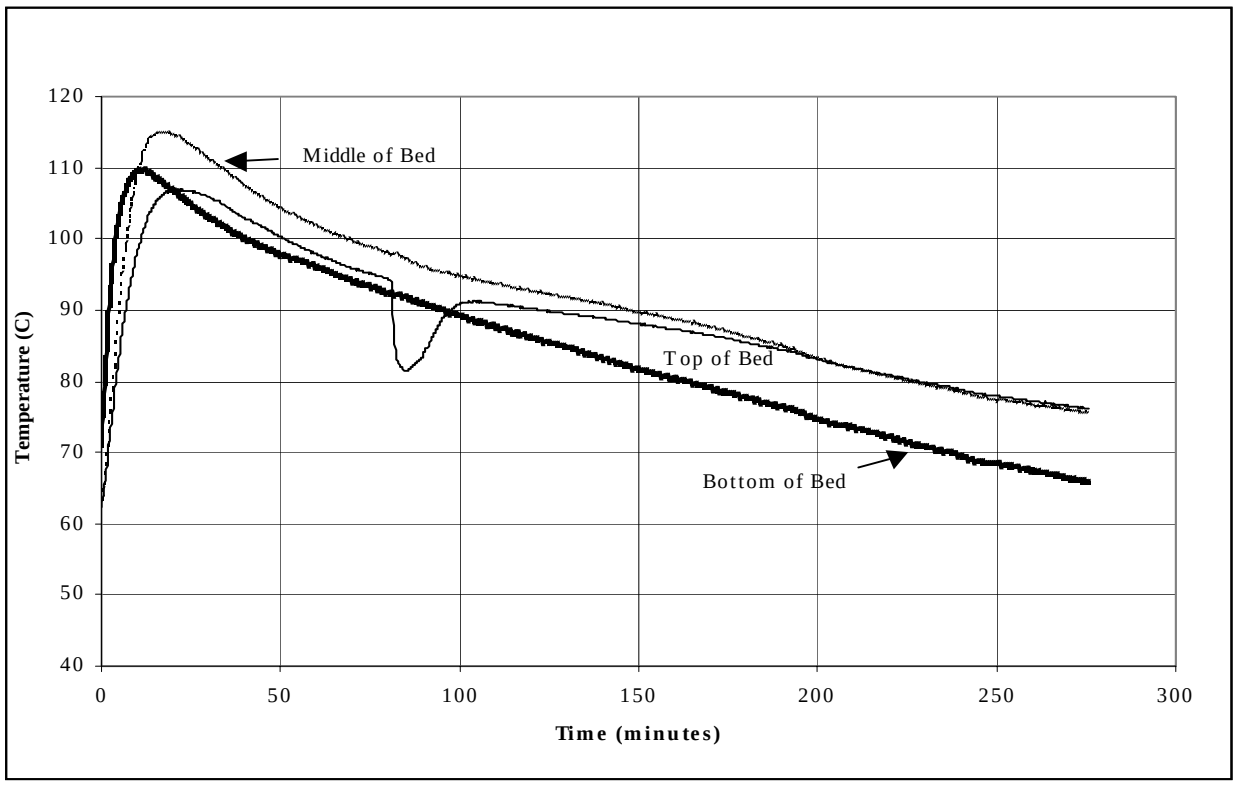

Figure 13. Temperature profile for fluidized bed carbonation of potassium carbonate.

4.5 Isothermal Thermogravimetry at RTI

4.5.1 Testing of Micronized Sodium Bicarbonate

Church and Dwight provided a sample of micronized sodium bicarbonate which was calcined in helium and then and then carbonated in 7.5% CO_2/5.9%H_2O. The initial carbonation took place to a minimal extent at 70°C, the temperature was then decreased to 60°C. The test data are shown in Figure 14.

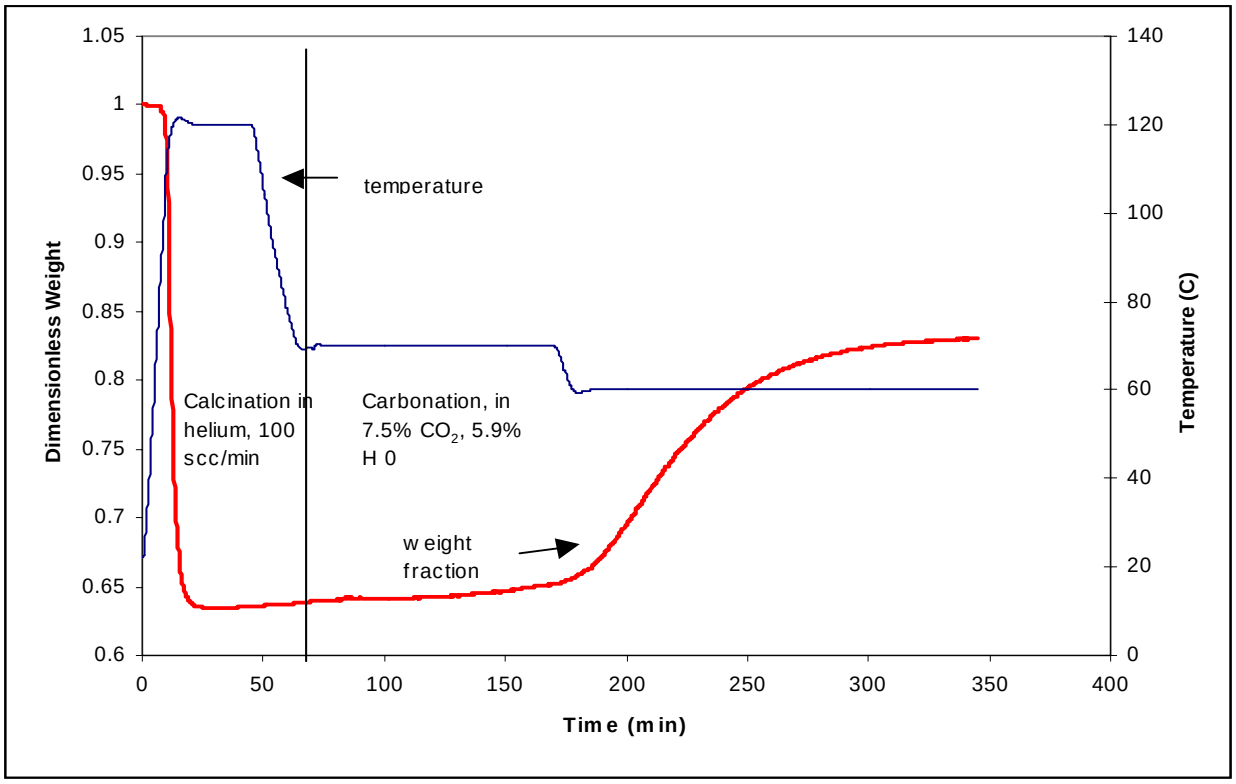

Figure 14. Calcination/carbonation of micronized sodium bicarbonate.

This finely divided material readily calcined in helium at 120°C to sodium carbonate. Subsequent carbonation at 70°C was quite slow with minimal weight gain over a two hour period. Upon lowering the temperature to 60°C, the carbonation took place at a comparable rate to the SBC grades with larger average particle sizes. The weight gain, after three hours at the lower temperature was approximately consistent with conversion of sodium carbonate to Na_2CO_3•3$NaHCO_3$, or Wegscheider's salt. This weight gain is consistent with what was observed with SBC #3.

4.5.2 Testing of Potassium Carbonate

Potassium carbonate was tested to determine its reactivity during carbonation and its capacity. Tests were conducted at 60, 80 and 100°C in an atmosphere of 7.5% CO_2/5.9% H_2O. Samples were dried in helium at 105°C before exposure to the carbonation gas to eliminate any

absorbed moisture. Weight gains, after 2 hours, approached 26%, 12% and 6% and 60, 80 and 100°C, respectively. This material may be useful at temperatures of 80°C and above, in contrast to Na_2CO_3, which has very little activity above 70°C. Test data are shown in Figure 15. It is also of interest that the initial rate of weight gain in the 80°C test was quite rapid, with about 75% of the apparent capacity used within the first 5 minutes of exposure to the carbonation gas.

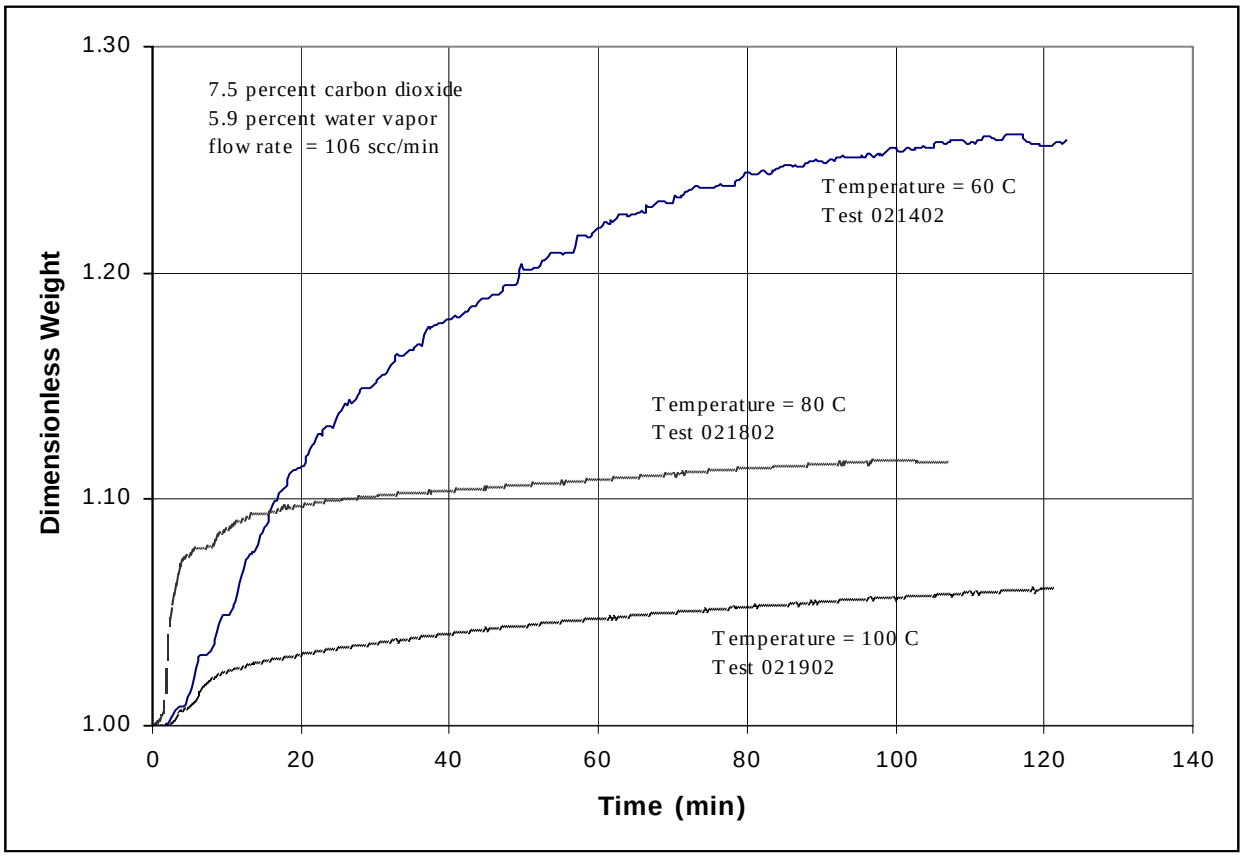

Figure 15. Carbonation of potassium carbonate.

The rates and extents of reaction of calcined SBC #3 and potassium carbonate are compared in Figure 16. At 60°C, the initial reaction rate for the calcined SBC #3 is slightly greater than that for the potassium carbonate. The calcined SBC #3 gains about 31% in weight over a two hour period. This approaches the stoiciometric weight gain of 35% that would result from complete conversion of sodium carbonate to Wegscheider's salt. Potassium carbonate gains about 26% in weight over the same period. This very closely approaches the stoiciometric weight gain that would result from complete conversion of potassium carbonate to the potassium analog of Wegscheider's salt, $K_2CO_3 \bullet 3KHCO_3$.

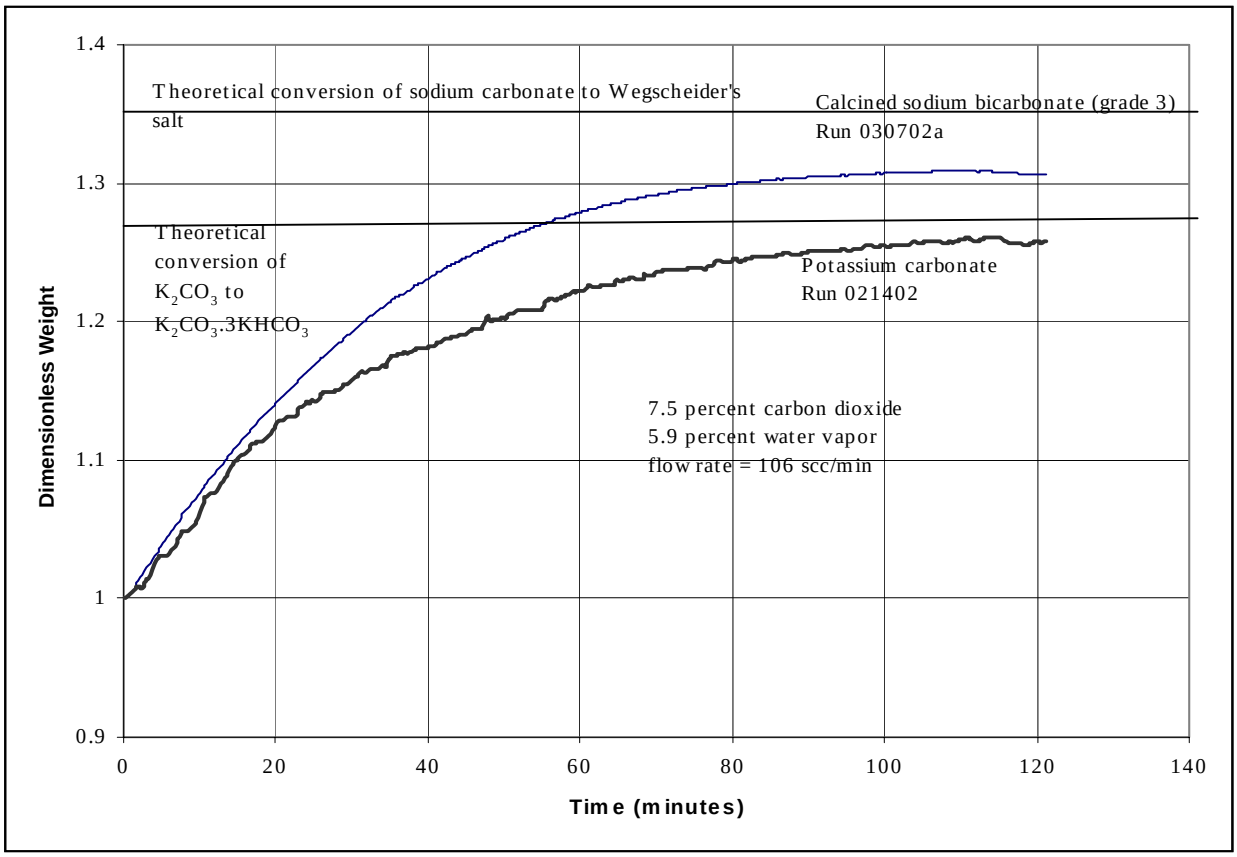

Figure 16. Carbonation of calcined SBC #3 and dried potassium carbonate at 60°C.

4.6 Heat Transfer Analysis and Nonisothermal Testing at RTI

In the January 2002 Quarterly Report (Green et al., 2002), it was proposed that the initial reaction rate of sodium carbonate with steam and carbon dioxide observed in the LSU TGA experiments was proportional to the difference between the equilibrium temperature for the carbonization reaction, evaluated at the bulk gas composition, and the bulk gas temperature. Thus

$$\text{Rate}_{\text{initial}} = \frac{dx}{dt}\Big|_{t=o} = h'(T_{eq} - T_b) \qquad (8)$$

where x is the conversion of sodium carbonate
t is the time, sec
h′ is a proportionality constant, $(K\ sec)^{-1}$
T_{eq} is the equilibrium temperature determined by thermodynamics at the bulk gas composition, K
and T_b is the bulk gas temperature, K.

The arguments for derivation of Equation (8) are based on theoretical considerations. The proportionality constant, h′, in Equation 8 can be shown to be

$$h' = \frac{hA_p}{N_o(-\Delta H)} \tag{9}$$

where h is the heat transfer coefficient between the external surface of the particle and the bulk gas, cal/(sec cm^2 K)
A_p is the external area of the particle, cm^2
N_o is the initial moles of Na_2CO_3 in the particle, gmol
and ΔH is the heat of reaction for the carbonization of the Na_2CO_3, cal/gmol Na_2CO_3

In the Quarterly Report (Green et al., 2002) it was shown that, for the limited number of experiments studied in detail, the results of the TGA sodium carbonate carbonization experiments were consistent with the formation of Na_2CO_3•3$NaHCO_3$ (Wegscheider's Salt) for experiments carried out at bulk gas temperatures of 70 to 80°C and the initial carbonization rate at a bulk gas temperature of 60°C was also consistent with the formation of Wegscheider's Salt. The TGA experiments at 60°C also showed that beyond the initial stages of carbonization, sodium bicarbonate may have also been formed. The results of the TGA carbonization experiments shown in Figure 17 were used to evaluate the parameters, T_{eq} and h′, contained in Equation 8. The best fit of the initial carbonization data was found to be given by

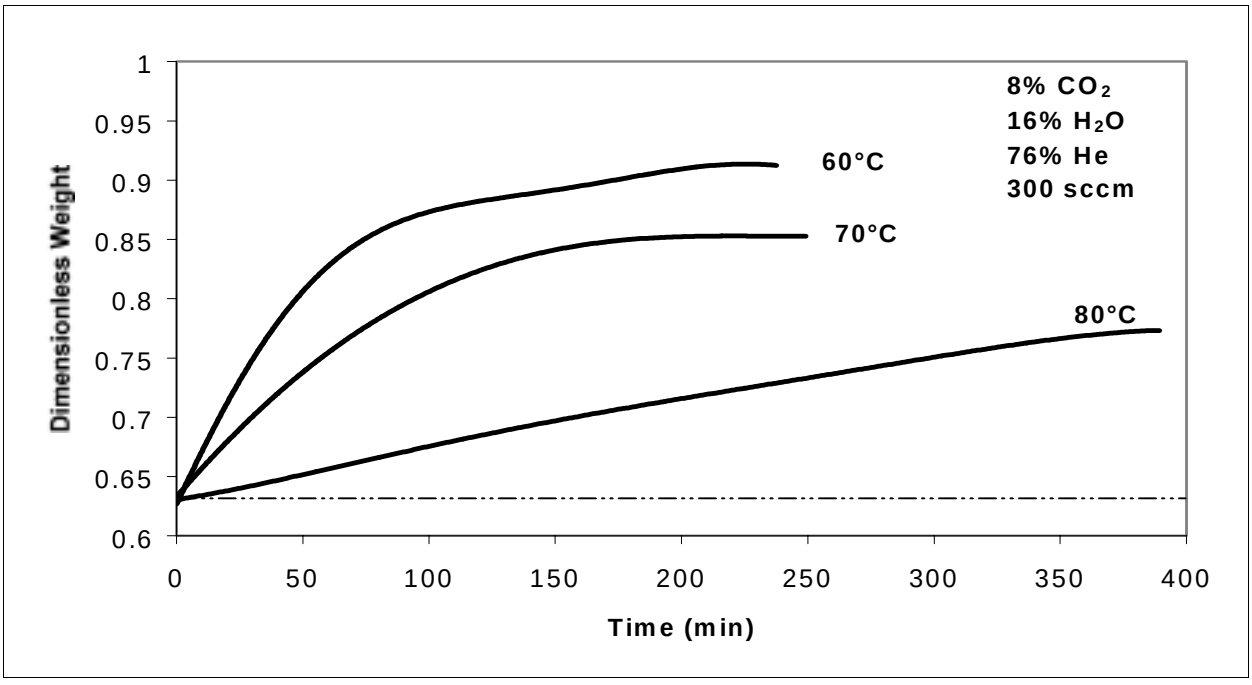

Figure 17. Effect of carbonation temperature using SBC grade #3 (for the formation of pure Na_2CO_3•3$NaHCO_3$ dimensionless weight should equal 0.85).

$$h' = 1.718 \times 10^{-5} (\text{sec } ^\circ\text{C})^{-1} \quad (10)$$

$$T_{eq} = 82.6\ ^\circ\text{C} \quad (11)$$

For the data shown in Figure 17, the partial pressures of CO_2 and water vapor upon where P_{CO2} = 0.08 atm and P_{H2O} = 0.16 atm, respectively. For this bulk gas composition, the equilibrium temperature, T_{eq}, of 82.6°C was found to be extremely close to the equilibrium temperature for the carbonization of Na_2CO_3 to Wegscheider's Salt as calculated by the HSC chemistry thermodynamics program, and as shown in Figure 18 which was previously reported by Green et al., January 2002. This equilibrium datum point is marked as "Equilibrium Data Point #1" in Figure 18.

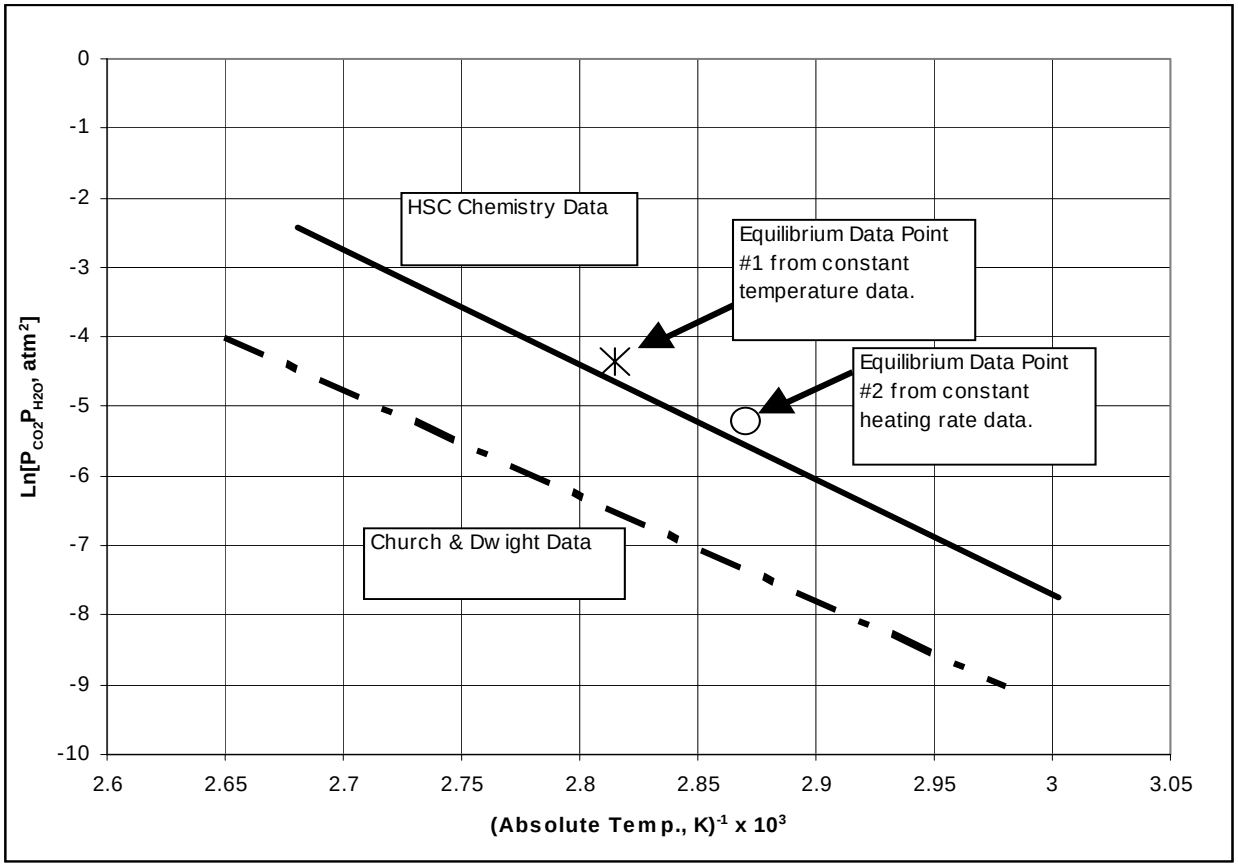

Figure 18. Comparison of equilibrium constants for the reaction: 2/3 Na_2CO_3•3$NaHCO_3$ ➔5/3 Na_2CO_3+ H_2O+CO_2, calculated from two sources of thermodynamic data.

The initial rates of carbonization of Na_2CO_3 for the TGA experiments summarized in Figure 17 were well correlated at low Na_2CO_3 conversion by the expression

$$-\ell n\,(1-\times) = kt \tag{12}$$

where k is a rate constant which is precisely equal to the initial rate of reaction. Applying Equation 12 to Equation 8 yields

$$\left.\frac{dx}{dt}\right|_{t=o} = k = h'\left(T_{eq} - T_b\right) \tag{13}$$

The carbonization data shown in Figure 17 were replotted in the form suggested by Equation 12 as shown in Figure 3. At each temperature, as shown in Figure 19, the least squares fit of the first four data points in the form suggested by Equation 12 were used to calculate the initial carbonization rate, k.

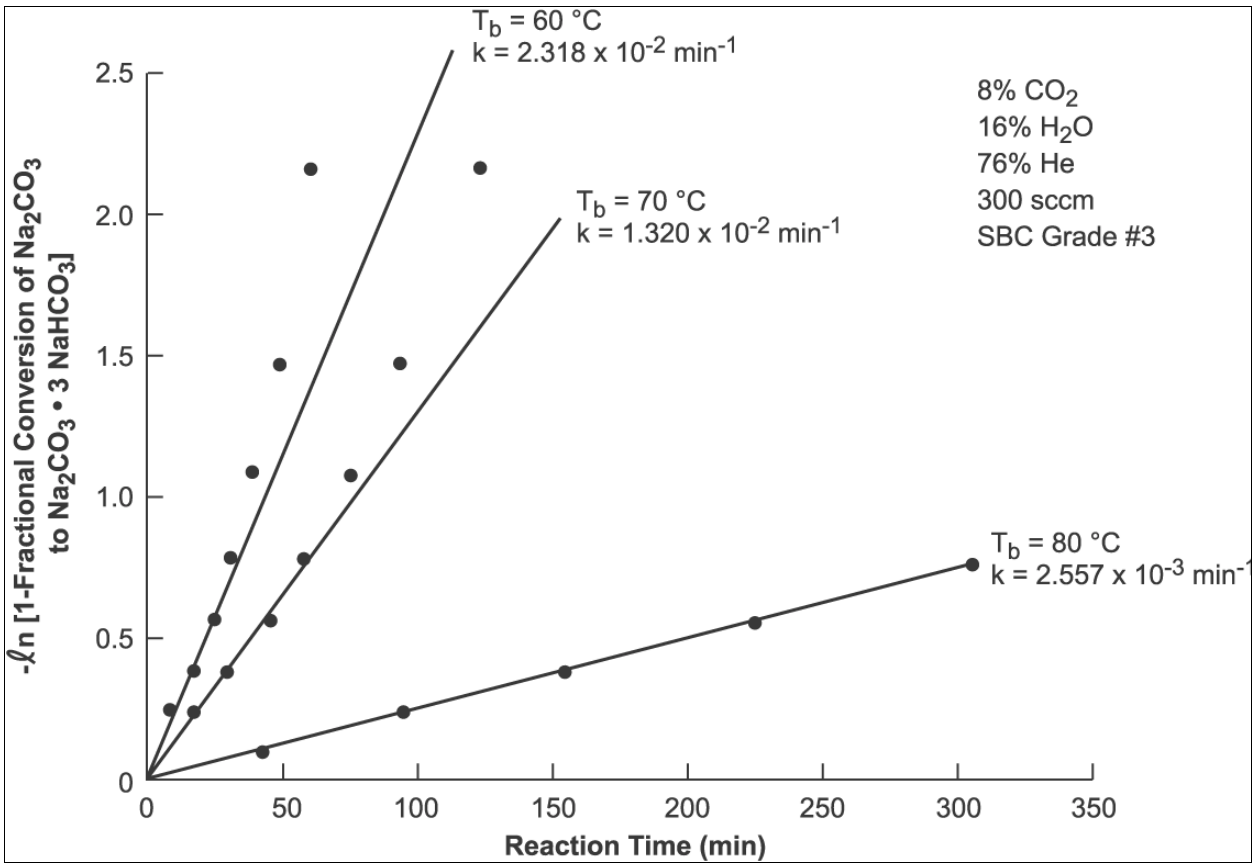

Figure 19. Carbonation rate data obtained from Figure 17.

The three resulting values of k (or the initial carbonization rates at the three bulk gas temperatures as shown in Figure 19) were then used to calculate the best values of parameters h' and T_{eq} via least squares fit of the data in the form given by Equation 13. The best values of the two parameters were given above by Equation 10 and 11. It can be seen from Figure 19

that the first order equation kinetics, given by Equation 12 can well represent the carbonization data up to conversions of 50 to 60%, but at higher conversions the carbonization data begin to significantly deviate from the first order reaction model described by Equation 12. Thus, if the parameters defining the factor h′ as given by Equation 9 can be evaluated and the equilibrium temperature can be calculated from thermodynamics, then the initial carbonization rate can be calculated via Equation 13, and the time required to obtain conversions of Na_2CO_3 to Wegscheider's Salt (up to 50% conversion) can then be calculated by Equation 12. On the other hand if conversions greater than 50% are involved, a more realistic model than the first order reaction model (Equation 12) of the carbonization process will be needed to estimate reaction times. One such model might involve a shrinking core of Na_2CO_3 in which the heat conduction from the core, through the newly formed Wegscheider's Salt layer, followed by the heat removal from the external surface (via forced convection) controls the carbonization rate.

4.6.1 Shrinking Core Model

RTI has developed a shrinking-core type model to simulate the carbonization of Na_2CO_3 in a roughly conical TGA cup. An idealization of this cup along with a few important dimensions is shown in Figure 20.

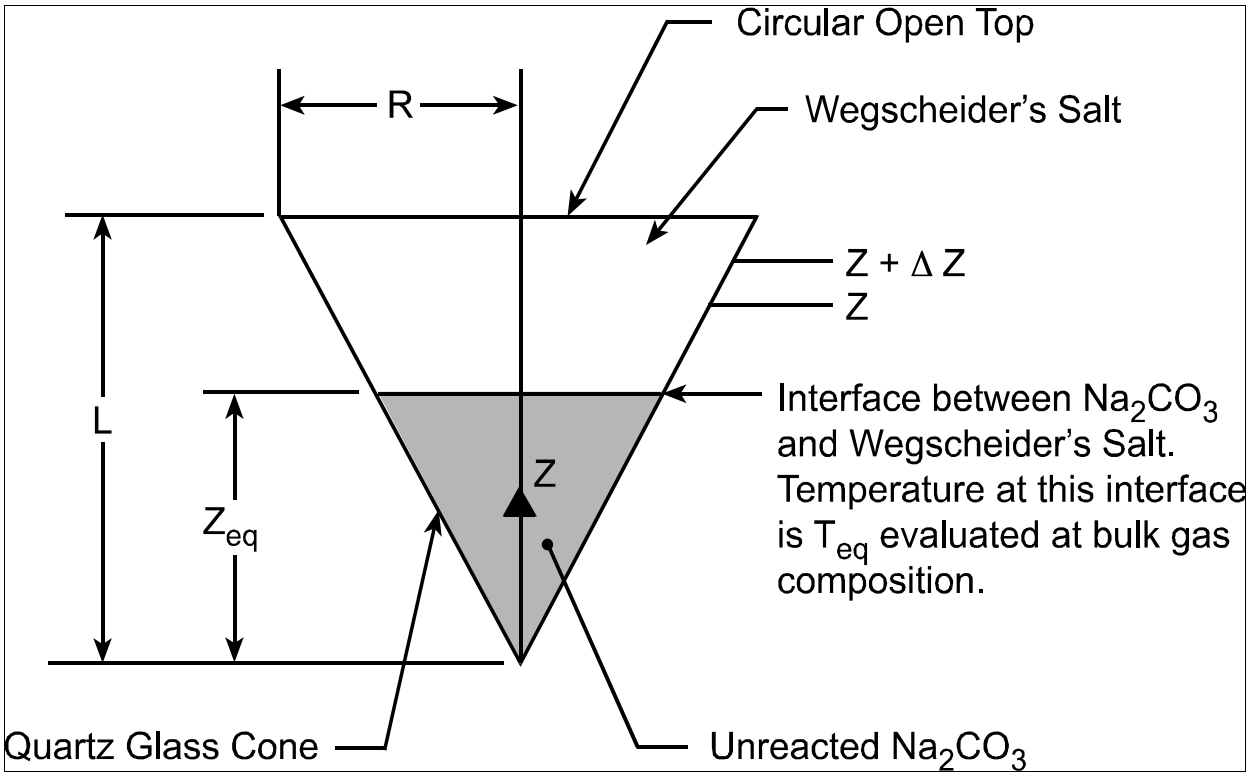

Figure 20. Idealized thermogravimetric analyzer sample cup.

As can be seen from Figure 20 the TGA cup is modeled as a cone with a circular base of radius R and a heigh of L. The distance, Z, is measured from the vertex of the cone. At some distance above the vertex, Z_{eq}, there is assumed to be an interface between the unreacted

Na_2CO_3 in the vertex of the cone and carbonized material in the upper portion of the cone. The temperature at this interface is assumed to be the equilibrium temperature determined by the equilibrium of the carbonization reaction evaluated at the bulk gas composition. This assumption would be valid under the condition

$$\frac{D_e\left(-\Delta H_{CO_2}\right)}{k_e} >> 1 \tag{14}$$

where k_e is the effective thermal conductivity of the carbonized Na_2CO_3, cal/(cm°C sec)
D_e is the effective diffusivity of CO_2 in the carbonized Na_2CO_3, cm^2/sec
ΔH_{CO2} is the enthalpy change for the carbonization reaction, cal/gmol CO_2

Under the conditions given by Equation 14, a small change in concentration of CO_2 within the carbonized material will give rise to very large change in temperature, and as a consequence, the equilibrium temperature at the unreacted-reacted Na_2CO_3 interface can be approximated by the equilibrium temperature evaluated at bulk gas partial pressures of CO_2 and water vapor.

In the shrinking core model of the conical TGA sample holder, carbon dioxide and water vapor diffuse from the bulk gas to the material interface located at a distance Z_{eq} above the vertex of the cone. The carbon dioxide and water vapor react at interface with unreacted Na_2CO_3 releasing a large amount of heat (roughly 31 Kcal/gmol CO_2 reacted). The temperature at the unreacted Na_2CO_3 interface will rise until the Na_2CO_3-Wegscheider Salt equilibrium temperature, T_{eq}, is reached. At this temperature the reaction becomes self extinguishing and temperature rise stops at T_{eq}. For further reaction to occur, heat must diffuse from the Na_2CO_3-Wegscheider's Salt interface, and thus the rate of carbonization will be limited by the transfer of heat from the interface. Some heat will be dissipated by simply heating the materials to the reaction temperature, T_{eq}; however the sensible heat effects amount to only a maximum of 5% of the heat released by chemical reaction and are ignored in the present model. The model also assumes that all reaction heat produced in the sample holder is lost through the open top of the holder. Any heat lost through the quartz holder is assumed to be small in comparison to the heat lost through the open top. This maybe reasonable in view of the fact that the quartz introduces a number of heat transfer resistances that do not exist at the open top.

The shrinking core model can be developed by carrying out a heat balance on slice of cone bounded from below by a disk at height Z and from above by a disk at height Z + ΔZ as shown in Figure 20; thus

$$q_z A\big|_Z - q_z A\big|_{Z+\Delta Z} = 0 \tag{15}$$

where q_z is the heat flux in the z–direction, cal/(cm^2sec)
A is cross-sectional area of the cone at height z

Note that the cross-section area, A, is a function of the height, Z, above the vertex. Using geometry,

$$A = \frac{\pi Z^2 R^2}{L^2} \tag{16}$$

Substituting Equation 16 into Equation 15 and simplifying gives

$$Z^2 q_Z\Big|_Z - Z^2 q_Z\Big|_{Z+\Delta Z} = 0 \tag{17}$$

Dividing Equation 17 by ΔZ and letting ΔZ→0 gives

$$\frac{d}{dz}\left(Z^2 q_Z\right) = 0 \tag{18}$$

Noting the heat flux, q_Z, is given by

$$q_Z = -k_e \frac{dT}{dz} \tag{19}$$

and substituting Equation 19 into Equation 18 yields

$$\frac{d}{dZ}\left(Z^2 k_e \frac{dT}{dZ}\right) = 0 \tag{20}$$

The boundary conditions are

$$T = T_{eq} \text{ at } Z = Z_{eq} \tag{21}$$

$$-k_e \frac{dT}{dZ} = h\left[T_L - T_b\right] \quad \text{at } Z = L \tag{22}$$

where T_L is the temperature at the open surface of conical sample holder, K.

The right-hand side of Equation (22) represents the convective heat removal from the open surface of the sample holder, and the quantity h is the convective heat transfer coefficient.

Integrating Equation (20) subject to the boundary conditions given by Equations 21 and 22 can be shown to give the following expression for the heat flux out of the open end of the cone:

$$\underset{\text{at } z = L}{\text{Heat Flux}} = -k_e \frac{dT}{dz}\Big|_{z = L} = \frac{\left(T_{eq} - T_b\right)}{\frac{1}{h} + \frac{L^2}{k_e}\left[\frac{1}{Z_{eq}} - \frac{1}{L}\right]} \tag{23}$$

This heat flux can also be related to reaction rate by the following expression

$$\underset{\text{at } z = L}{\text{Heat Flux}} = \frac{N^O_{Na_2CO_3}\left[(-\Delta H)\right]}{\pi R^2}\frac{dx}{dt} \tag{24}$$

where $N^o_{Na_2CO_3}$ is the initial moles of Na_2CO_3 in the conical sample holder, gmol

and ΔH is the enthalpy of reaction, cal/gmol Na_2CO_3

Noting that,

$$N^{o}_{Na_2CO_3} = \frac{\pi R^2 L}{3}\rho \tag{25}$$

where ρ is the initial bulk density of the Na_2CO_3 in the cone, gmol/cm^3, and substituting Equations 24 and 25 into Equation 23 gives

$$\frac{L\rho(-\Delta H)}{3}\frac{dx}{dt} = \frac{(T_{eq} - T_b)}{\frac{1}{h} + \frac{L^2}{k_e}\left[\frac{1}{Z_{eq}} - \frac{1}{L}\right]} \tag{26}$$

Rearranging gives

$$\left[1 + \frac{hL}{k_e}\left(\frac{L}{Z_{eq}} - 1\right)\right] dx = \frac{3h(T_{eq} - T_b)}{(-\Delta H)\rho L}dt \tag{27}$$

Equation 27 can be integrated subject to appropriate initial conditions, if Z_{eq} can be related to the Na_2CO_3 conversion, x. This can be done through consideration of the geometry of the sample holder; thus

$$\frac{Z_{eq}}{L} = (1 - x)^{1/3} \tag{28}$$

Substitution of Equation 28 into Equation 27 yields an integrable equation relating conversion to reaction time. Thus

$$\left[1 + \frac{hL}{k_e}\left\{(1 - x)^{-1/3} - 1\right\}\right] dx = \frac{3h(T_{eq} - T_b)dt}{(-\Delta H)\rho L} \tag{29}$$

It is interesting to note that according to Equation 29, the conversion, x is <u>not</u> a function of the cone radius, R. Integrating Equation 29 subject to the initial condition

$$x = 0 \text{ at } t = 0 \tag{30}$$

gives

$$x + \frac{hL}{k_e}\left[\frac{3}{2} - \frac{3}{2}(1 - x)^{-2/3} - x\right] = \frac{3h(T_{eq} - T_b)}{(-\Delta H)\rho L}t \tag{31}$$

It can be noted that the conversion, x, is a function only of the dimensionless parameter, hL/k_e, and a dimensionless time represented by the right-hand side of Equation 31.

The general equation, Equation 29, relating conversion to reaction time for the shrinking core-type model for the conical sample holder geometry, is exactly the same as the equation that would be derived for the shrinking core model for spherical geometry, except in the spherical geometry case, the height of the cone, L, in Equation 29 would be replaced by the radius of the sphere.

Equation 31 can be useful in interpreting the TGA data shown in Figure 17. Since the data taken at 60°C, as shown in Figure 17, involves the reaction of Wegscheider's Salt to sodium bicarbonate at high reaction times, these data do not meet the reaction conditions assumed in the derivation of Equation 31. Therefore it is not suitable for the interpretation of the 60°C data on Figure 17 (except the data at low reaction time which are consistent with the formulation of Wegscheider's salt). The carbonization data at 80°C on Figure 17 involve only low conversions. Therefore, the data at 70°C in Figure 17, which involve a full range of conversion up to 100% Na_2CO_3 to Wegscheider's salt, appear to be a good test of the shrinking core model. Based on the 70°C TGA carbonization data in Figure 17, the parameter

$$\beta = \frac{hL}{k_e} \tag{32}$$

and the time scale factor

$$\alpha = \frac{3h(T_{eq} - T_b)}{(-\Delta H)\rho L} \quad [=] \sec^{-1} \tag{33}$$

which appear in Equation 31, can be evaluated. Then, those two factors can be used in Equation 31 to calculate reaction times for given experimental conversions and finally the calculated reaction times can be compared with the experimental reaction times below.

In order to calculate the best values of α and β that would tend to minimize the difference between computed and experimental reaction times, Equation 31 can be rearranged as follows:

$$\alpha^{-1}x + \left(\frac{\beta}{\alpha}\right)\left[\frac{3}{2} - \frac{3}{2}(1-x)^{-2/3} - x\right] = t \tag{34}$$

The least squares values of α^{-1} and β/α can be found by the minimization of the following function, S, which respect to α^{-1} and β/α :

$$S = \sum \left(t_i^c - t_i^e\right)^2 \tag{35}$$

where t^c_i is the calculated reaction time based on the experimentally observed conversion, x_i, sec
t^e_i is the experimentally observed reaction time at the experimentally observed conversion, x_i, sec

Substituting Equation 34 into the above equation gives

$$S = \sum \left[\alpha^{-1} x_i + \frac{\beta}{\alpha}\left(\frac{3}{2} - \frac{3}{2}\left(1 - x_i\right)^{2/3} - x_i \right) - t_i^e \right]^2 \quad (36)$$

The values of α and β which minimized the sum of the squares of the differences between calculated and experimentally observed reaction times, s are

$$\alpha = 2.150 \times 10^{-4} \text{ sec}^{-1} \quad (37)$$

$$\beta = 2.675 \quad (38)$$

The ability of the shrinking core model to fit the TGA data and be able to predict reaction times at high conversions is shown in Table 3. In this table, it can be seen that the shrinking core model, as represented by Equation 31, does an excellent job of predicting reaction times. In the least squares determination of the parameters α and β, the seven experimental data points corresponding to conversion of 0.2045 through 0.8864, as shown in Table 3, were used in the determination as described above. The data point at 100% conversion was not used; yet if the calculated and experimentally measured reaction times at 100% conversion are compared as in Table 3, it can be seen that the agreement in the two reaction times is almost exact. Thus, it would appear that the shrinking core model would be an excellent tool in analyzing the TGA carbonization data. In comparison, as shown Table 3, the use of the first order carbonization model, Equation 12, to extrapolate initial rate, low conversion data to higher conversion falls apart at conversion of roughly 50%; and at 66% conversion there is approximately 12% error in the reaction time prediction.

Recently RTI has been encouraged by its collaborator, Church and Dwight, to attempt to study the carbonization kinetics of Na_2CO_3 using constant heating rates in the TGA. This method is described in detail in the ASTM Standard E1641. Basically a sample of material is decomposed at a given constant heating rate in a TGA and the fractional decomposition as a function of time and temperature are recorded. A series of four or more experiments are carried out at different heating rates. At a given fixed percent decomposition (less than 20%) the temperature at which the fixed decomposition is reached is determined as a function of heating rate. These data are then plotted as the natural logarithm of the heating rate verses the reciprocal absolute temperature at which the given fixed percent decomposition is reached. The slope of this line is then the negative of activation energy of the decomposition reaction divided by the ideal gas constant.

RTI has carried out a series of TGA carbonization experiments at constant heating rates of 0.1, 0.2, 0.5 and 1.0 K/min. The results of these experiments are shown in Figures 21 through 24, respectively. In these experiments approximately 20 mg of SBC #3 was calcined to Na_2CO_3 at 150°C in a helium atmosphere. The carbonate was cooled to 55°C in helium at which time a gas containing CO_2 and water vapor at partial pressure of 0.0753 and 0.0587 atm, respectively, was introduced into the TGA. The balance of the gas was nitrogen and oxygen. In the reactive carbonizing gas the samples of calcined SBC #3 were heated to 80°C at the given constant heating rates. As can be seen in Figures 21 through 24, the dimensionless weight, or equivalently the conversion of Na_2CO_3 to possibly Wegscheider's salt, show a maximum. An understanding of why this is so can be obtained from the shrinking core model given by Equation 29. Equation 29 can be rewritten in the form

Table 3. Comparison of the Experimentally Measured Reaction Times and Reaction Times Computed Using Various Models.

From 70°C curve of Figure 17		Calculated Reaction Times (min)	
Experimental conversion, X	Experimental Reaction Time, t, min	Shrinking Core Model, Equation 31, with 60 $\alpha = 1.290 \times 10^{-2}$, min, and $\beta = 2.675$	First Order Initial Rate Extrapolation, Equation 12 with $K = 60\ h'\ (T_{eq} - T_b)$ $h' = 1.718 \times 10^{-5}$ $(\sec\ °C)^{-1}$ $T_{eq} = 82.6°C$
0	0	0	0
0.2045	16.7	17.5	17.6
0.3182	29.3	28.8	29.5
0.4318	42.9	41.6	43.5
0.5455	56.5	56.4	60.7
0.6593	74.2	73.9	82.8
0.7727	92.0	94.9	114.0
0.8864	124.4	123.0	167.3
1.0000	180.6	181.2	∞

$$f(x,\beta)\frac{dx}{dt} = h'(T_{eq} - T_b) \tag{39}$$

where

$$h' = 3h / \left((-\Delta H)\rho L\right) \quad [=] \quad (°C\ \sec)^{-1} \tag{40}$$

and

$$f(x,\beta) = 1 + \beta\left\{(1-x)^{-1/3} - 1\right\} \tag{41}$$

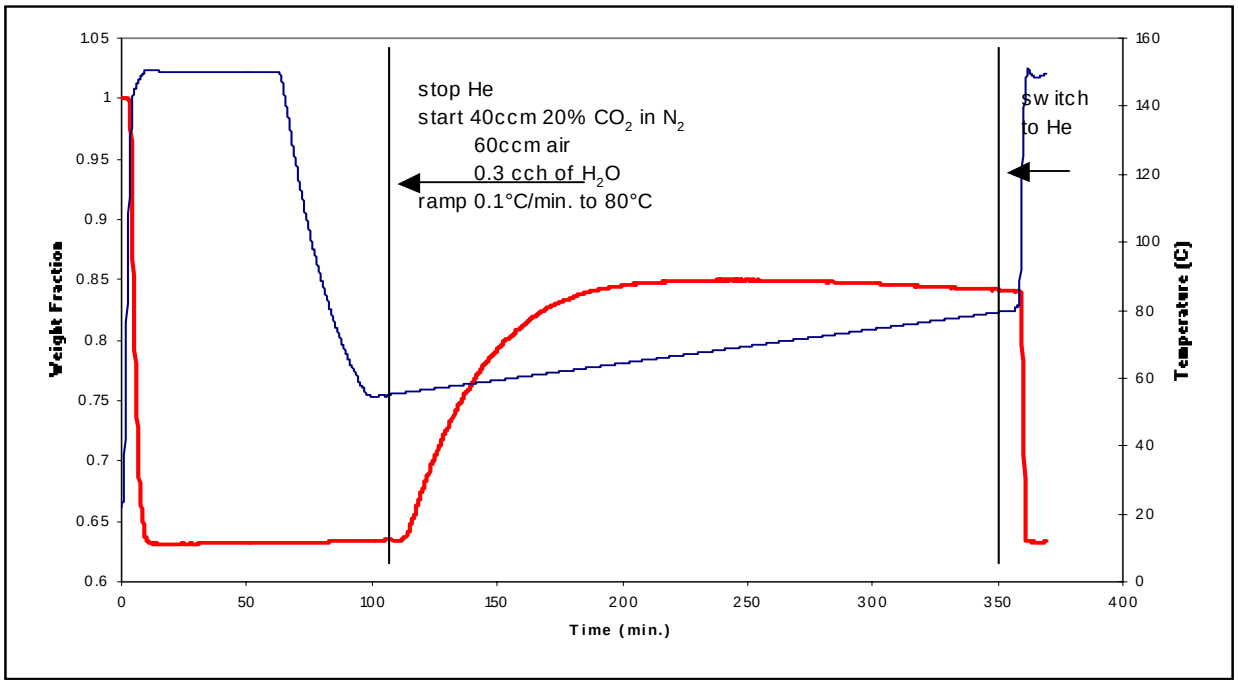

Figure 21. Carbonation of SBC #3 at constant heating rate of 0.1°C/min.

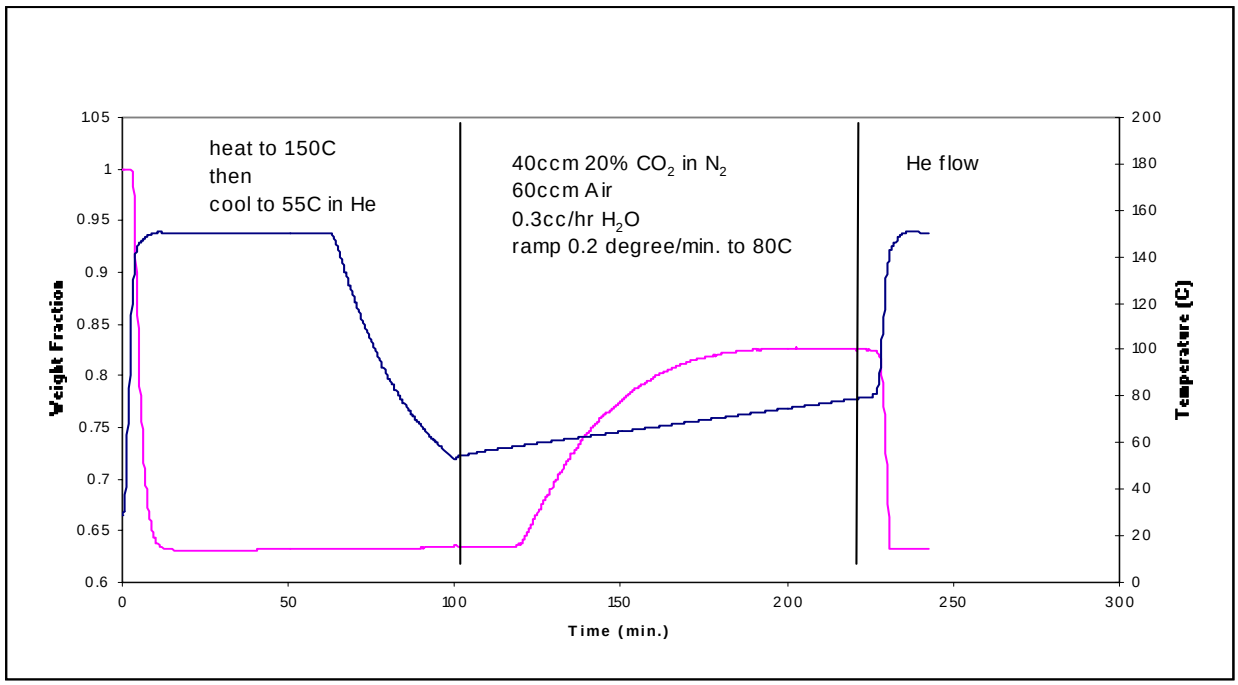

Figure 22. Carbonation of SBC #3 at constant heating rate of 0.2°C/min.

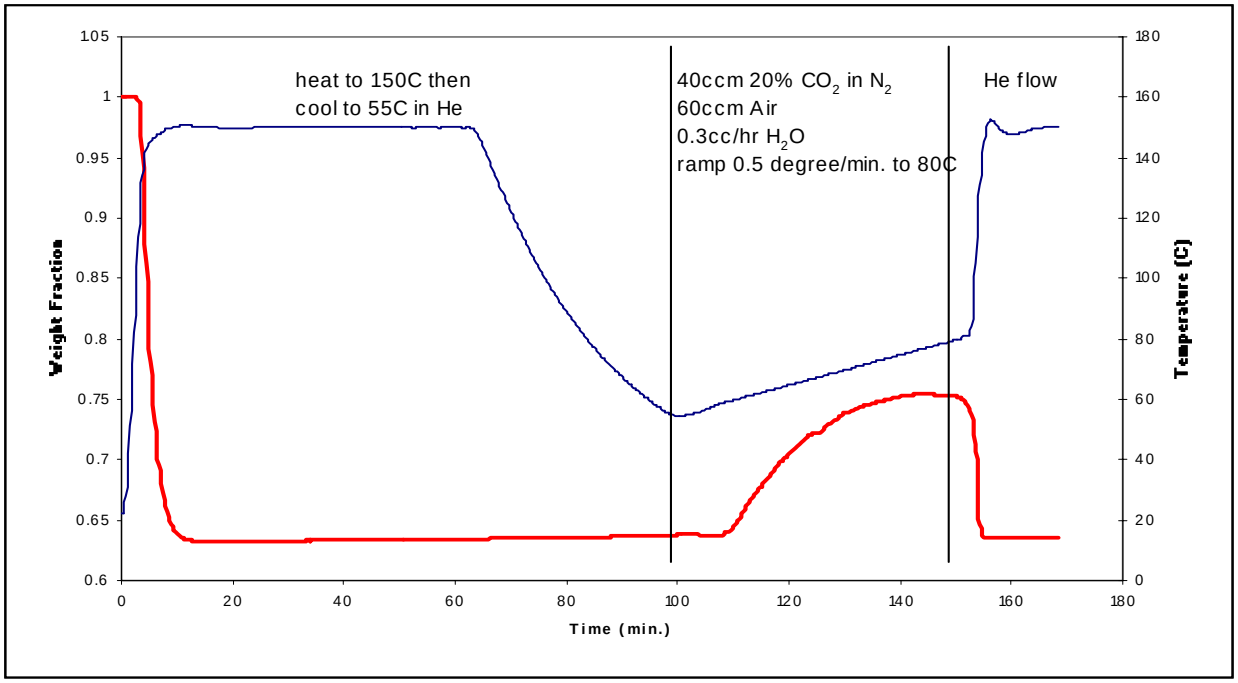

Figure 23. Carbonation of SBC #3 at constant heating rate of 0.5°C/min.

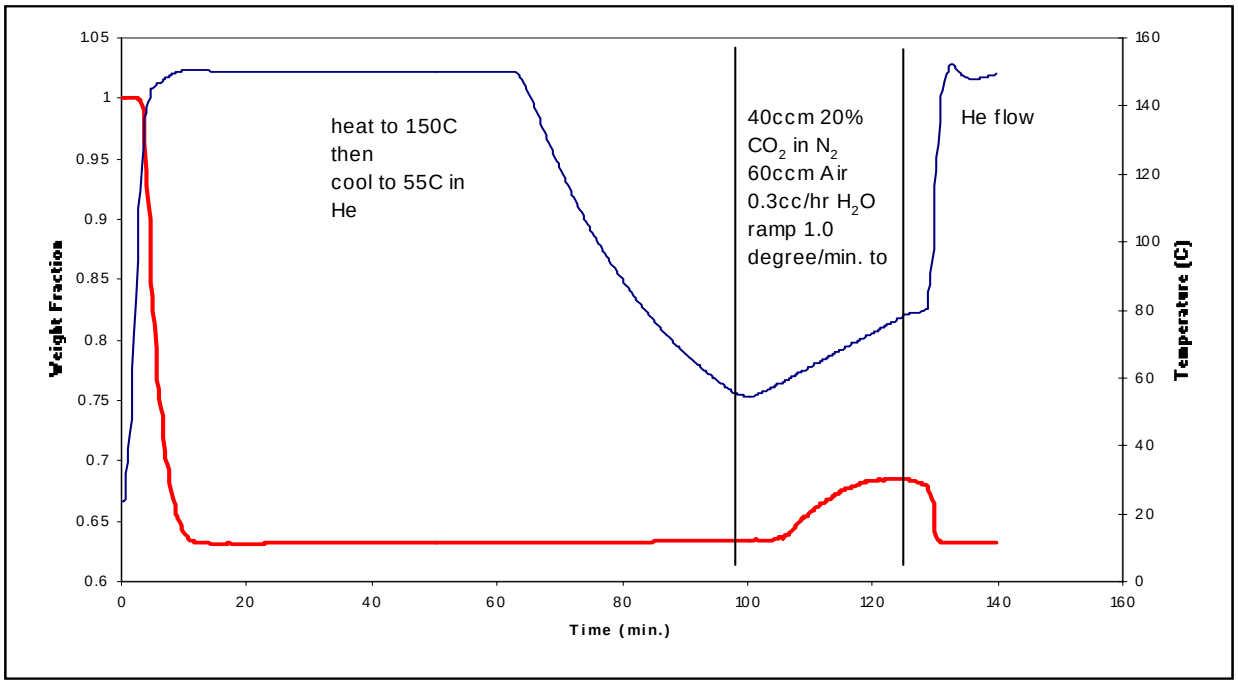

Figure 24. Carbonation of SBC #3 at constant heating rate of 1.0 °C/min.

It can be seen from Equation 39 that if the range of bulk gas temperature, T_b, used in the constant heating rate experiments encompasses the equilibrium temperature, T_{eq}, the conversion, x, should have a maximum with respect to reaction time when the bulk gas temperature and the equilibrium temperature are equal, since under this condition, the first derivative of the conversion, x, with respect to reaction time equals zero:

$$\frac{dx}{dt} = 0 \tag{42}$$

Thus, the constant heating rate experiments can be used to quickly estimate the equilibrium temperature for the carbonization reaction. For the four experiments shown in Figures 21 through 24 the equilibrium temperatures at the various heating rates are shown in Table 4.

As can be seen in Table 4 the agreement between the various estimates values of the equilibrium temperature is fairly good except for the value obtained at a heating rate of 0.1K/min. Examination of Figure 21 for the 0.1K/min heat rate experiment, shows that the conversion at the end of the heating rate period is very flat making it difficult to pick out a single point at which the maximum in the conversion occurred. Ignoring the 0.1 K/min experiment, the average equilibrium temperature based on the other three experiments is 75.9°C for $\ell n\ P_{CO2}P_{H2O} = \ell n\ (0.0753 \times 0.0587) = -5.42$.

Table 4. Estimated Equilibrium Temperatures, T_{eq}, Obtained in Four Heating Rate Experiments Summarized in Figure 5 Through 8

Heating Rate K/min	Estimated Equilibrium Temperature, T_{eq}
0.1	69.8
0.2	75.6
0.5	76.5
1.0	75.6

This information has been plotted on the equilibrium curves shown in Figure 18 and is marked “Equilibrium Data Point # 2". As in the case for the equilibrium point calculated from the least squares fit of the initial rate data obtained from the constant bulk gas temperatures shown in Figure 17, the present equilibrium point calculated using constant heating rate data agrees reasonably well with the equilibrium curve calculated by HSC Chemistry for the Na_2CO_3 - Wegscheider’s salt system.

The shrinking core model described above and summarized by Equation 29 should be useful in correlating the carbonization data obtained from the four constant heating rate experiments summarized in Figures 21 through 24. Under conditions of constant heating rate the bulk gas temperature in the TGA is given by

$$\frac{dT_b}{dt} = \gamma \tag{43}$$

subject to $T_b = T_{bo}$ at $t = t_o$

where γ is the heating rate, K/min or °C/min

t_o is an arbitrary time which occurs after the start of weight gain in the carbonization curves, min.

T_{bo} is the bulk gas temperature, °C, at the chosen time, t_o

Integrating Equation 43 gives

$$T_b = T_{bo} + \gamma\,(t - t_o) \tag{44}$$

Substituting this equation into Equation 29 gives

$$\left[1 + \beta\left\{(1 - X)^{-1/3} - 1\right\}\right]dx = h'\left[\left(T_{eq} - T_{bo}\right) - \gamma\left(t - t_o\right)\right]dt \tag{45}$$

where

$$\beta = \frac{hL}{k_e} \tag{46}$$

$$h' = \frac{3h}{(-\Delta H)\rho L} \quad [=] \quad \left(^{\circ}C\ min\right)^{-1} \tag{47}$$

Equation 45 can be integrated subject to

$$x = x_o \text{ at } t = t_o \tag{48}$$

where x_o is the conversion of Na_2CO_3 to Wegscheider's salt at the chosen time, t_o.

This integration gives

$$\beta\left[\frac{3}{2}\left[\left(1 - x_o\right)^{\frac{2}{3}} - \left(1 - x\right)^{-\frac{2}{3}}\right] - \left(x - x_o\right)\right] + \left(x - x_o\right) = h'\left[\left(T_{eq} - T_{bo}\right)\left(t - t_o\right) - \frac{\gamma}{2}(t - t_o)^2\right] \tag{49}$$

Defining the functions

$$G\left(x, x_o, \beta\right) = \beta\left[\frac{3}{2}\left[\left(1 - x_o\right)^{\frac{2}{3}} - \left(1 - x\right)^{\frac{2}{3}}\right] - \left(x - x_o\right)\right] + \left(x - x_o\right) \tag{50}$$

and

$$\tau\left(t, t_o, T_{eq}, T_{bo}\right) = \left[\left(T_{eq} - T_{bo}\right)\left(t - t_o\right) - \frac{\gamma}{2}\left(t - t_o\right)^2\right] \tag{51}$$

Equation 49 reduces to

$$G = h'\tau \tag{52}$$

Thus, the conversion data produced in the constant heating rate experiments, if plotted in the form suggested by Equation 52, should be on a straight line passing through the origin and having a slope equal to h'. Figure 25 shows such a graph. The conversion data for heating

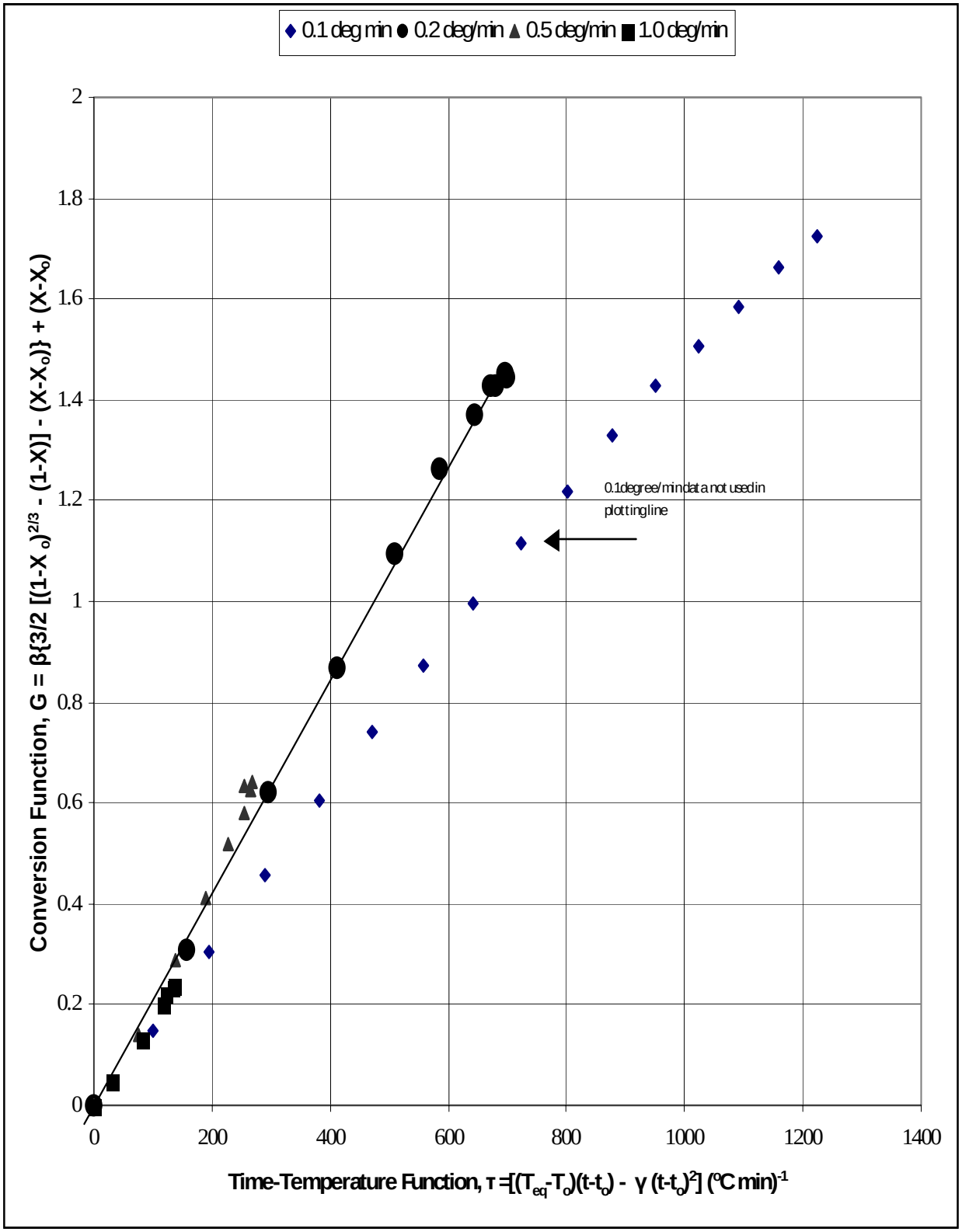

Figure 25. Extent of carbonation of Na_2CO_3 to Wegscheider's salt as a function of time for the constant heating rate experiments.

rates of 0.2, 0.5 and 1.0°C/min seems fairly consistent as graphed in Figure 25 in that the functions G and τ roughly lay on a straight line; however, the data for the 0.1°C/min heating rate experiment is not consistent with the data obtained in the other three experiments. The reason for this anomaly is not known at this time. It should be noted that the equilibrium temperature T_{eq}, obtained from the experiment carried out at a heating rate of 0.1°C/min was also inconsistent with the equilibrium temperatures obtained from the experiments carried out at 0.2, 0.5 and 1.0°C/min as demonstrated previously in Table 4. The equilibrium temperature used to calculated Time-Temperature function, τ, shown in Figure 25, was the average of the equilibrium temperatures obtained from the 0.2, 0.5 and 1.0°C/min experiments. Table 5 summarizes the values of the various parameters used in calculating the functions G and τ and in constructing Figure 25.

Table 5. Parameters Use in Constructing Figure 25

∝, Heat Rate °C/min	Equilibrium Temperature, T_{eq} °C	Initial Time, t_o min	Gas Temperature at $t=t_o$. °C	Conversion at $t=t_o$
0.1	75.9	114.0	55.8	0.0343
0.2	75.6	120.3	58.9	0.0338
0.5	76.5	109.5	60.1	0.0781
1.0	75.6	106	59.1	0.0283

Based on the ability of the shrinking core model, described above, to fit conversion data as a function of reaction time from both constant temperature and constant heating rate TGA experiments, the model appears to be promising for correlating kinetic data from the TGA Na_2CO_3 carbonation experiments. Whether this model and correlations can be extended to conditions encountered by particles in other reactor systems, such as the fast fluidized bed, and how that could be done, is not known at this time.

Returning to the ASTM standard E1641 for determining the activation energy, E, for a first order decomposition of the form

$$\frac{dx}{dt} = Ae^{-E/RT}(1-x) \tag{53}$$

where x is the extent of decomposition
A is the frequency factor, min^{-1}
E is the Arrhenius activation energy, cal/gmol
R is the ideal gas constant, 1.987 cal/(gmol κ)
T is the decomposition temperature, κ
t is time, min

Using the data given in Figures 21 through 24 for the constant heating rate experiments, Table 6 can be constructed

Table 6. Temperatures Corresponding to 20% Conversion.

γ, Heating Rate °C/min	Temperature, °C, at which x = 0.20
0.1	56.4
0.2	60.1
0.5	61.9

These data are plotted in Figure 26 as suggested by ASTM Standard E1541. The slope of curve shown in Figure 26 should be

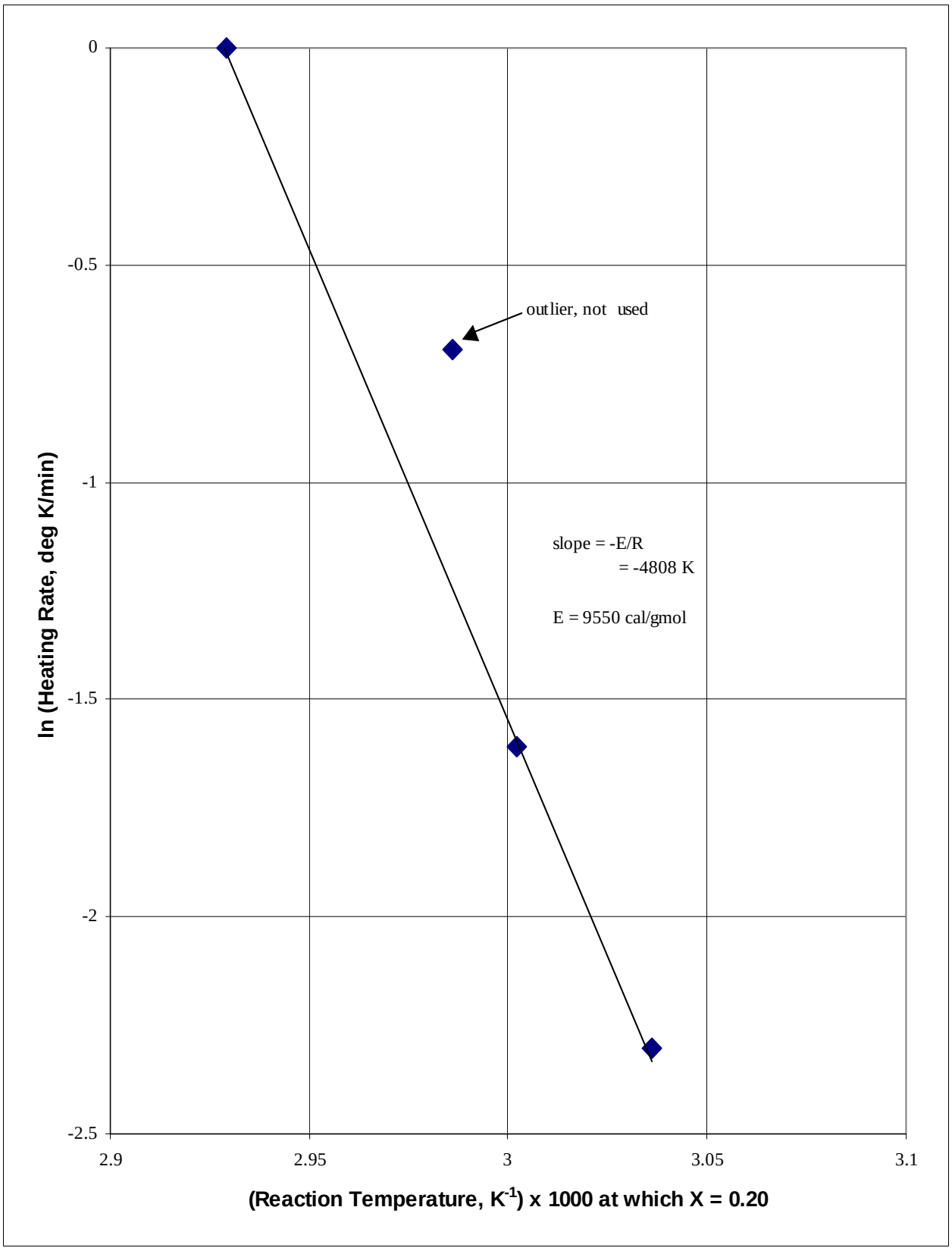

Figure 26. Determination of decomposition activation energy by means of ASTM E1541.

$$\text{slope} = -E/R \quad [=] \quad K \tag{54}$$

Based on the data in Figure 26, the activation energy, E, is roughly +9550 cal/gmol. This implies, as a result of Equation 53, that the conversion rate of Na_2CO_3 via reaction of Na_2CO_3 with CO_2 and water vapor should increase with increase in temperature whereas the TGA data shown in Figure 17 of this report shows the conversion rate of Na_2CO_3 clearly decreases with increase in temperature. The resolution of this discrepancy is of concern, but not yet available.

5.0 CONCLUSIONS AND FUTURE WORK

Exposure of calcined SBC #3 to water vapor prior to contact with carbonation gas does not significantly increase reaction rates in electrobalance testing.

Calcined trona T-200 has a greater initial reaction rate than calcined SBC #3, and an equivalent carbon dioxide capacity. It appears that T-200 is more susceptible to increased calcination temperatures than SBC #3, in terms of both initial reaction rate and capacity.

In fixed bed reactor testing of SBC #3, 50 to 60 percent of the carbon dioxide was removed from simulated flue gas during the initial 80 minutes of testing.

Results of Davison Attrition Index determinations suggested that SBC #5, commercial grade sodium carbonate and extra fine granular anhydrous potassium carbonate were unsuitable, as tested, for entrained reactor processing.

In fluidized bed testing of potassium carbonate, 35% of carbon dioxide was removed from simulated flue gas in the initial stages. Carbon dioxide removal declined to 6% at the point that the sorbent capacity was 54% exhausted. This material was much more prone to caking and plugging of the fluid bed than calcined SBC #3. Potassium carbonate appears to continue to react with carbon dioxide at higher temperatures than calcined SBC #3.

In TGA carbonation reactions at 60°C, calcined SBC #3 approaches a weight gain consistent with formation of Wegscheider's salt. Potassium carbonate, tested under the same conditions, approaches a weight gain consistent with formation of the potassium analog of Wegscheider's salt ($K_2CO_3 \bullet 3KHCO_3$).

A shrinking core model can be used to explain carbonation times in electrobalance experiments.

Nonisothermal TGA data at heating rates between 0.2 and 1.0°C/minute imply that the activation energy for reaction of sodium carbonate with carbon dioxide and water is +9550 cal/gmole.

In the coming quarter, RTI will produce spray dried potassium carbonate on a durable support for fluid bed testing. LSU will continue to improve the fixed bed reactor system and develop a procedure that will insure that steam is present when CO_2 reaches the sorbent. LSU will repeat

five-cycle tests using trona to determine if the first test results can be duplicated. Church and Dwight will subject fixed bed reactor samples to examination by X-ray diffraction and scanning electron microscopy.

6.0 REFERENCES

ASTM, International, Method D5757-95: Standard Test Method for Determination of Attrition and Abrasion of Powdered Catalysts by Air Jets. 1995

ASTM, International, Method E1641-99: Standard Test Method for Decomposition Kinetics by Thermogravimetry. 2000.

Green, D.A., Turk, B.S., Gupta, R., and Lopez Ortiz, A., Carbon Dioxide Capture From Flue Gas Using Dry Regenerable Sorbents, Quarterly Technical Progress Report, Research Triangle Institute, January 2001(a).

Green, D.A., Turk, B.S., Gupta, R., Lopez Ortiz, A., Harrison, D.P., and Liang, Y., Carbon Dioxide Capture From Flue Gas Using Dry Regenerable Sorbents, Quarterly Technical Progress Report, Research Triangle Institute, May 2001(b).

Green, D.A., Turk, B.S., Gupta, R., McMichael, Harrison, D.P., and Liang, Y., Carbon Dioxide Capture From Flue Gas Using Dry Regenerable Sorbents, Quarterly Technical Progress Report, Research Triangle Institute, January 2002.